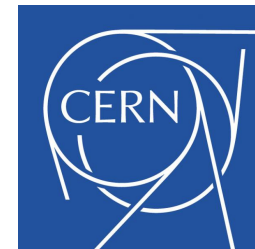


Intensity-dependent effects in the Accelerator Test Facility 2 and extrapolation to future electron-positron linear colliders

P. Korysko
University of Oxford
CERN



Outline

- Intensity-dependent effects in ATF2
 - Simulations
 - * Impact of static imperfections.
 - * Impact of dynamic imperfections.
 - * Impact of corrections (One-to-one, DFS, WFS)
 - Measurements
 - * Impact of corrections (DFS, WFS, wakefield knobs).
 - * Comparison between simulations and measurements.
- Impact of short-range and long-range wakefields in the 380 GeV CLIC BDS.
- Impact of short-range and long-range wakefields in 500 GeV ILC BDS.
- Conclusions

The Accelerator Test Facility (ATF2)

ATF2 layout, Twiss and parameters

ATF2 is a test facility to study the feasibility of the Final Focus System [1] that is envisaged in the future linear colliders CLIC and ILC. The primary project goal is to establish the hardware and beam handling technologies pertaining to transverse focussing of the electron beams to 37 nm. All the parameters can be found in the ATF2 design proposal report [2].

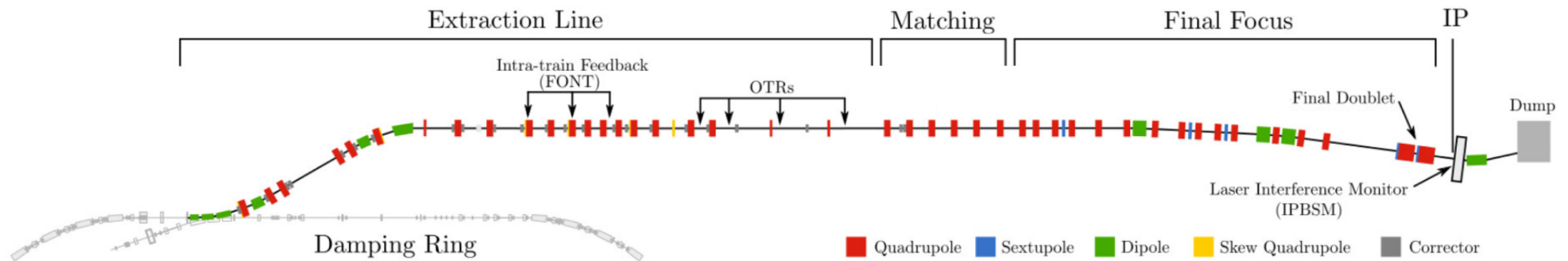
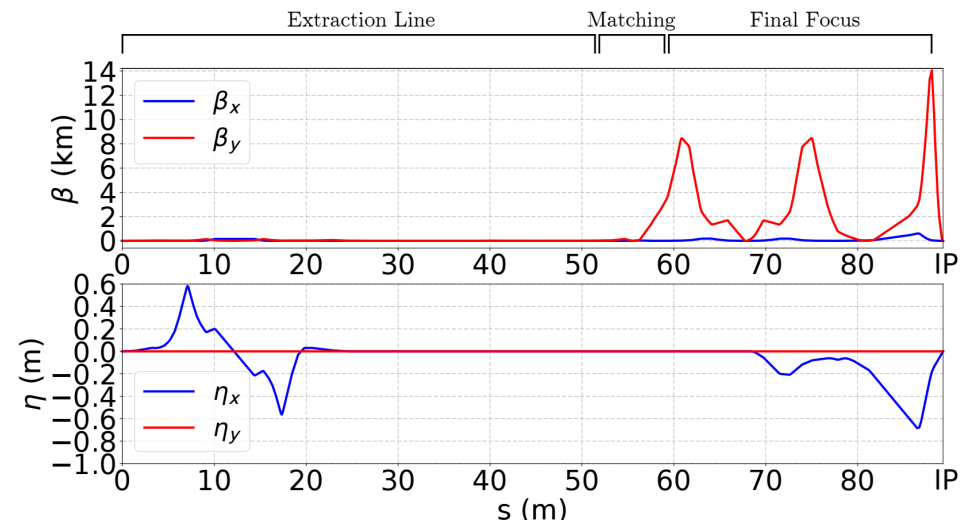


Table : Beam and optics parameters for ATF2 beamline.

Parameter	Symbol	Value
Length of ATF2	L	90 m
Beam energy	E	1.28 GeV
Bunch population	N_e	1.0×10^{10}
Beta functions at IP	β_x^*/β_y^*	40 mm/0.10 mm
Beam sizes at IP	σ_x^*/σ_y^*	8.9 μm /37 nm
Bunch length	σ_z	7 mm



Bunch length measurement

Previous measurements

Goals of ATF2

The ATF2 beamline was designed and built in order to fulfill two goals:

- Goal 1: Achieve a small vertical beam size at the IP (37 nm) and demonstrate the efficiency of the Final Focus System based on local chromaticity correction;
- Goal 2: Control the beam position and demonstrate the efficiency of the beam orbit's stabilisation with a nanometer precision at the IP.

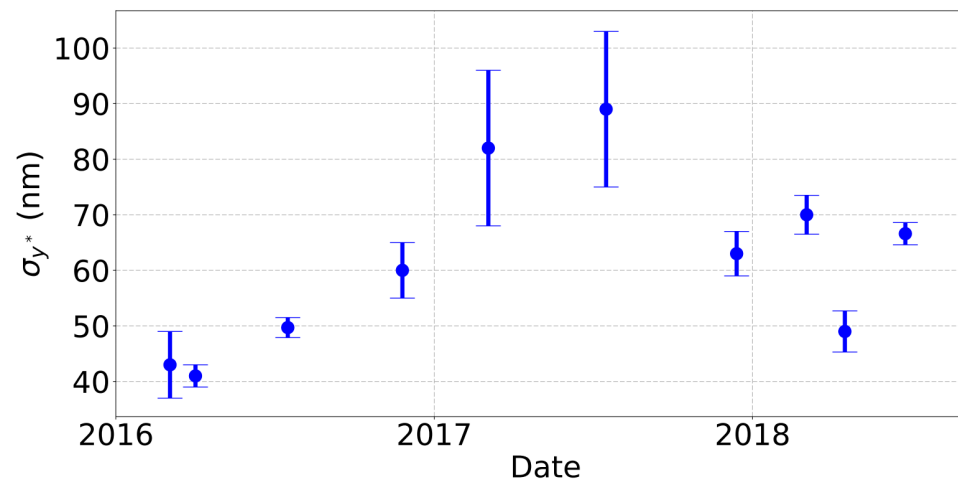


Figure: The ATF2 vertical IP beam size measurement history.

All small beam sizes were obtained with a beam intensity of $[0.5-1.5] \times 10^9$ e⁻/bunch

Intensity-dependent effects in ATF2 Simulations

Wakefield introduction

Introduction

Transverse and longitudinal wakefields

The integrated fields seen by a test particle traveling on the same, or on a parallel path at a constant distance s behind a point charge Q are called the integrated longitudinal and transverse wakepotentials. They are defined as:

$$\tilde{W}_{\perp}(\Delta r, s) = \frac{1}{Q} \int_0^L [E_{\perp}(\Delta r, z, s) + c\hat{z} \times B(\Delta r, z, s)] dz$$

$$\tilde{W}_{\parallel}(s) = -\frac{1}{Q} \int_0^L [E_z(z, s)] dz$$

The transverse and longitudinal kicks felt by a particle, at position z along the bunch, due to all leading particles ($\forall z' : z' > z$):

$$\Delta r' = \frac{\Delta P_{\perp}}{P} = \frac{qQL}{Pc} \int_{-\infty}^z W_{\perp}(\Delta r(z'), z - z') \rho(z') dz'$$

$$\Delta P_{\parallel} = \frac{qQL}{c} \int_{-\infty}^z W_{\parallel}(z - z') \rho(z') dz'$$

with:

- $\rho(z')$ normalized line charge density of the bunch, such that $\int_{-\infty}^{\infty} \rho(z') dz' = 1$
- $\Delta r(z')$ transverse radial position of the leading particles as a function of their position z' along the bunch [mm]
- Q total charge of the bunch [C]

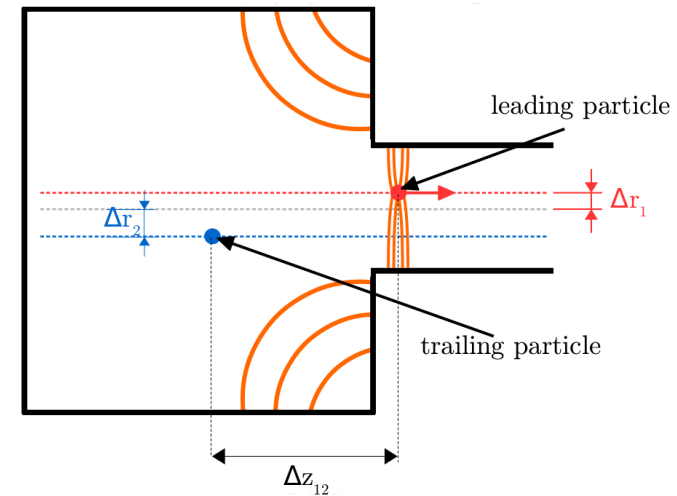


Figure: Scheme of the two-particle model.

- q particle's charge [e]
- P particle's momentum [eV/c]
- $\Delta r'$ radial kick [rad]
- ΔP momentum loss [eV]

Intensity-dependent effects in ATF2 Simulations

Impact of corrections

CLIC orbit correction (1/3)

One-to-one correction

The One-to-one correction consists of minimizing the transverse position of the beam, with respect to the beam pipe centre measured at BPMs, using steering magnets [3].

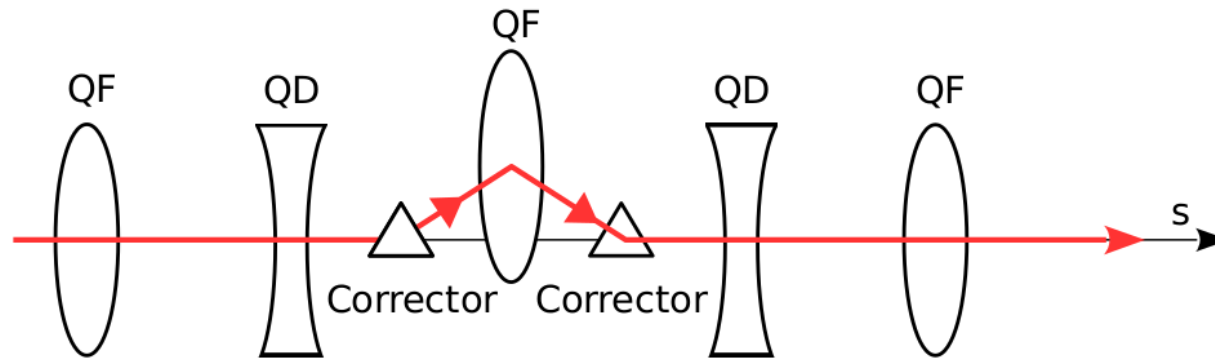


Figure: Schematic of the One-to-one correction. The beam orbit (in red) is deflected by correctors (triangles) in order to pass through the center of the BPM, which is inside a quadrupole in this case.

CLIC orbit correction (2/3)

Dispersion Free Steering (DFS) correction

In the simulations, two beams are tracked with two different energies, E_1 and E_2 . Steering magnets are then used to correct the orbit and reduce the orbit difference between the two beams $\Delta_{y,E}$ [4].

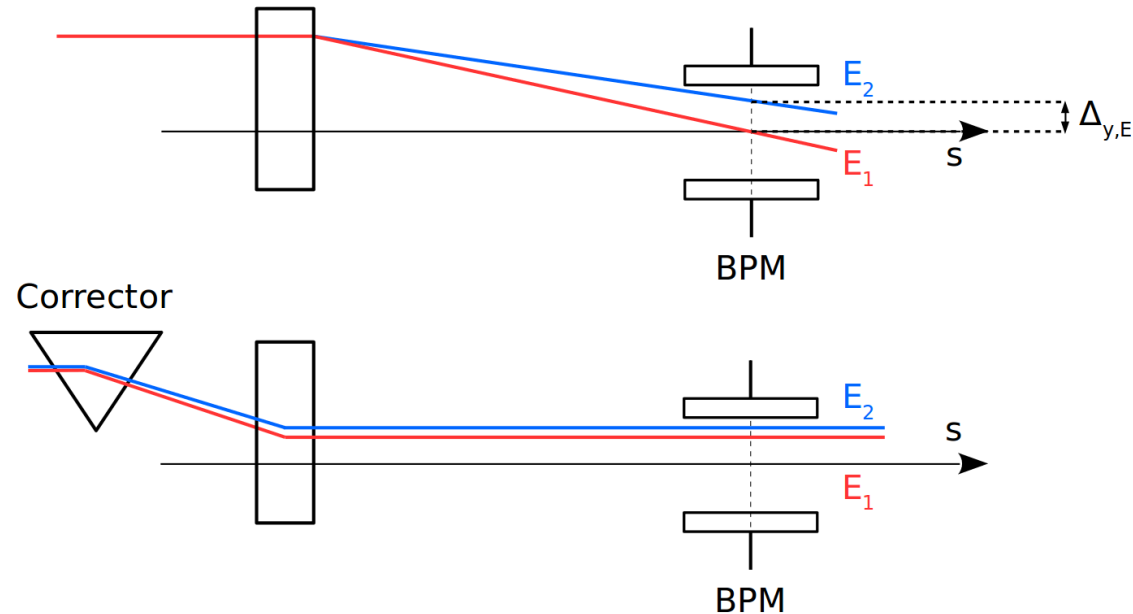


Figure: Schematic of the Dispersion Free Steering correction.

CLIC orbit correction (3/3)

Wakefield Free Steering (WFS) correction

The Wakefield Free Steering is an algorithm which corrects the difference on the orbit introduced by wakefields. In the simulations, two beams are tracked with two different charges Q_1 and Q_2 . Steering magnets are then used to correct the orbit and reduce the orbit difference between the two beams $\Delta_{y,Q}$ [5].

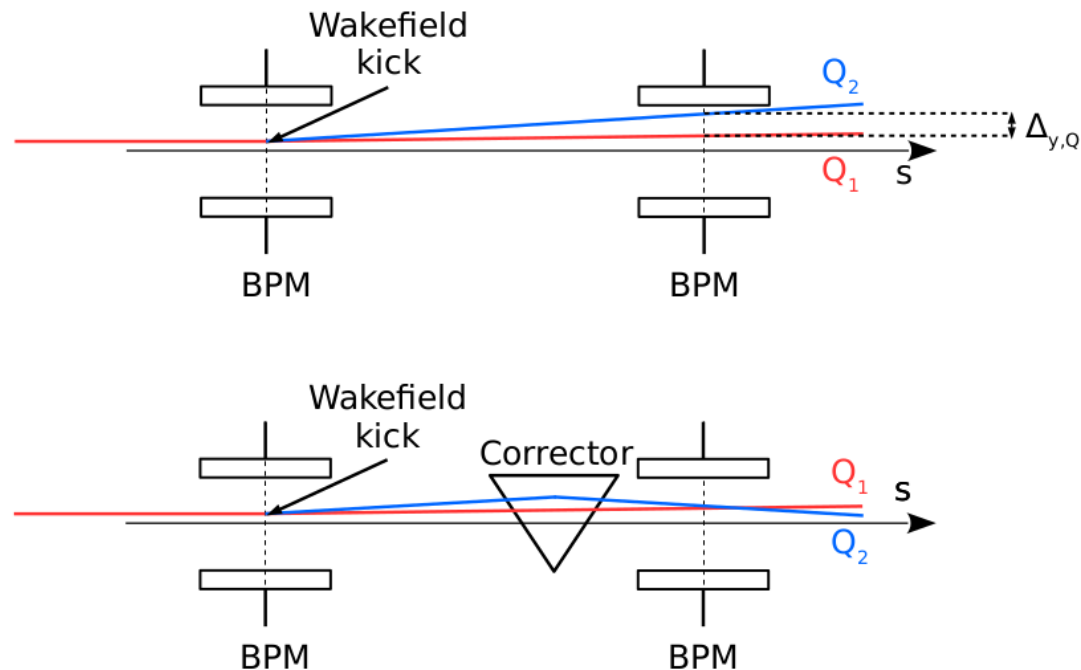


Figure: Schematic of the Wakefields Free Steering corrections.

Sextupole knobs

- First order knobs correction by changing the position of final focus sextupoles.
- Second order knobs correction by changing the strength of the final focus sextupoles.

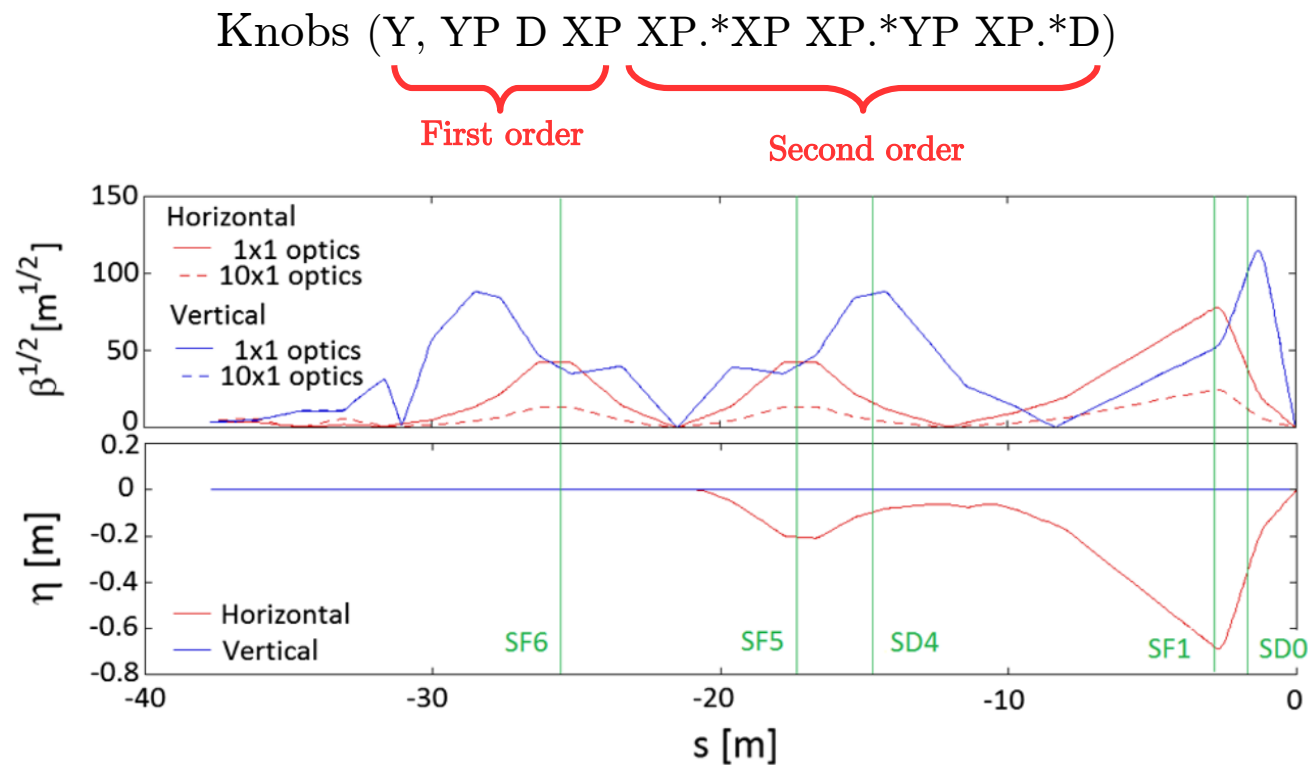


Figure: Positions of the sextupole knobs in the Accelerator Test Facility 2 (ATF2) [6].

Impact of corrections in ATF2

Simulation conditions (1/2)

Simulated errors:

- Static errors:
 - Misalignment of quadrupoles, sextupoles, BPMs of 100 μm RMS.
 - Strength error of quadrupoles, sextupoles of 0.01% RMS.
 - Roll error for quadrupoles and sextupoles of 200 μrad RMS.

Corrections applied:

- One-to-one
- DFS
- WFS
- Knobs (Y, YP D XP XP.*XP XP.*YP XP.*D)

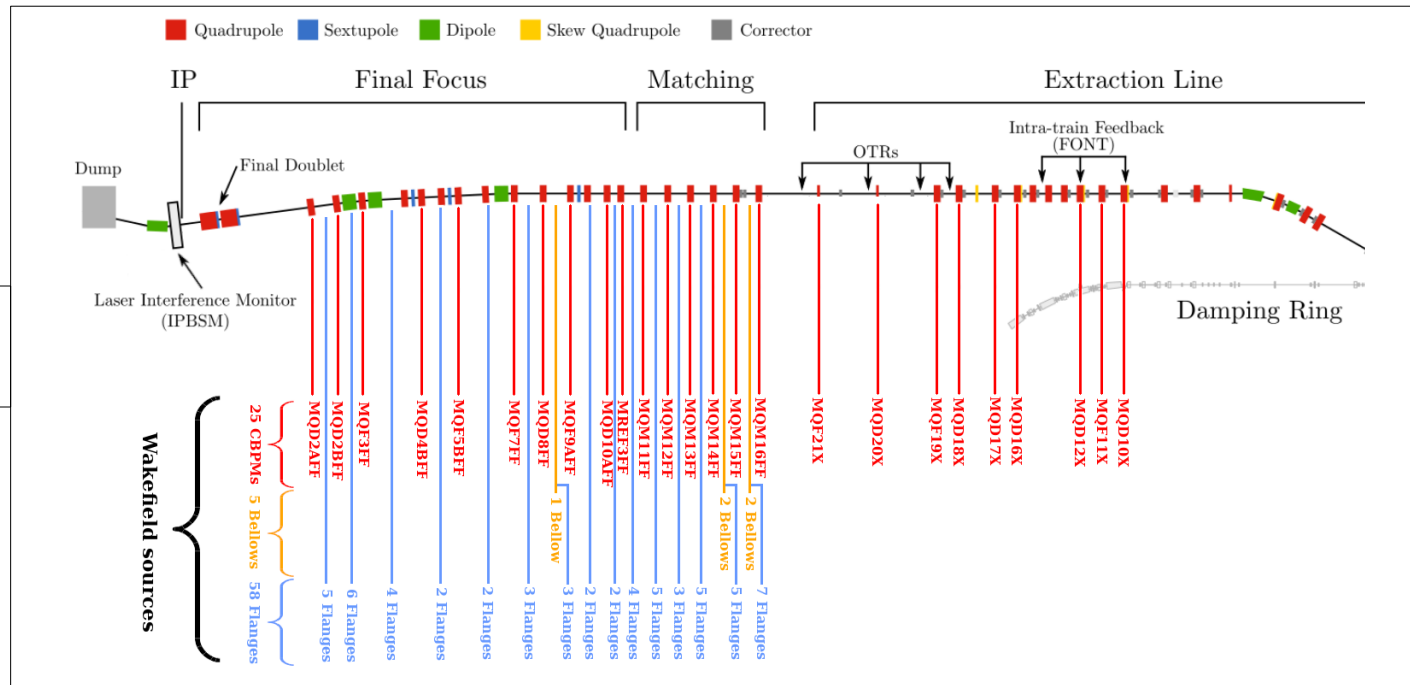

Simulation procedure:

- 100 machines with the previously cited static imperfections.
- Apply the cited corrections and the knobs on the distribution at the IP.
- Measure the vertical beam size at the IP.

Impact of corrections in ATF2 Simulation conditions (2/2)

Wakefield sources: Cavity BPMs, bellows and flanges (wakepotentials calculated with GdfidL). [7][8][9]

Position of
wakefield sources

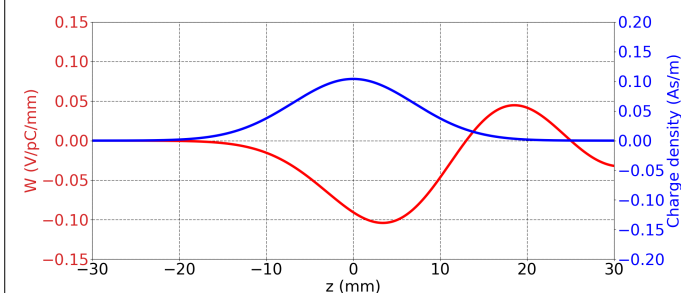
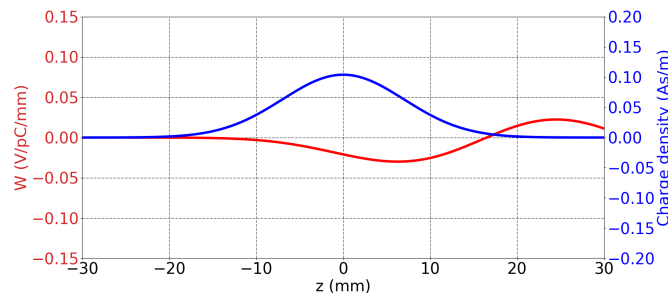
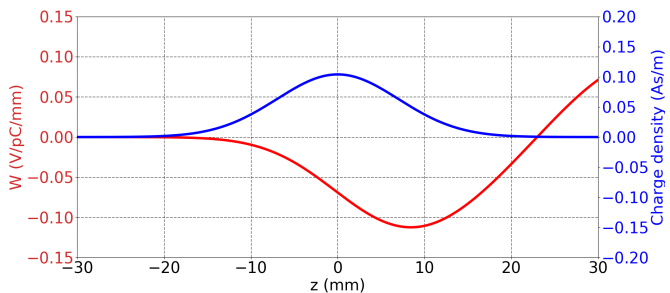


Wakefield sources wakepotentials (V/pC/mm)

Cavity BPM

Bellows

Flange



Impact of orbit corrections in ATF2

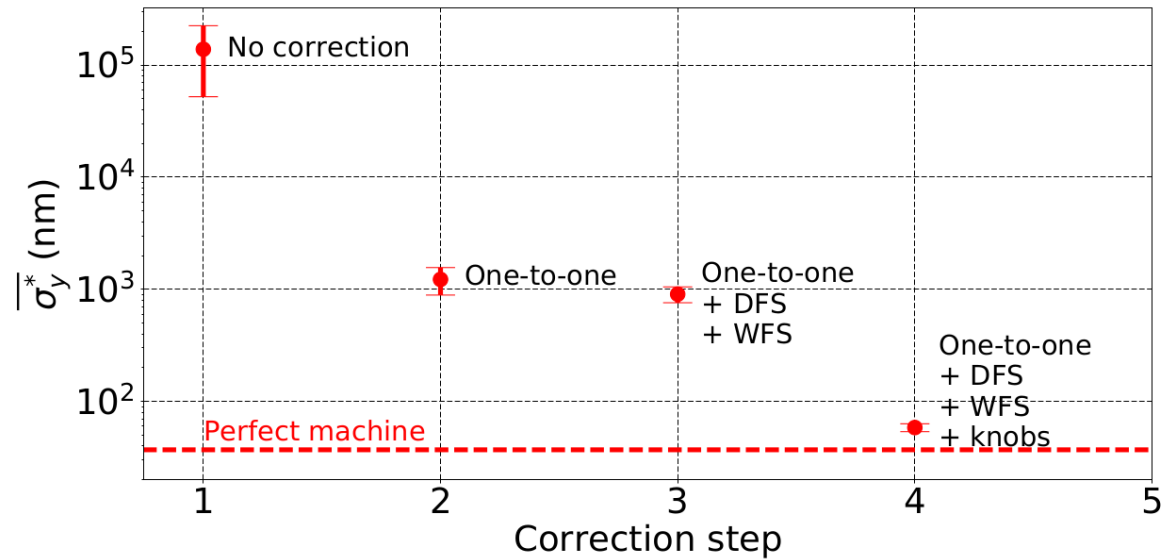


Figure : Average vertical beam size at the IP (σ_y^*) vs. correction step: One-to-one, DFS, WFS corrections and IP tuning knobs. The red dashed line show the vertical beam size at the IP for a perfect machine, 37 nm.

Correction	$\overline{\sigma_y^*}$
No correction	$13.8 \pm 86.2 \mu\text{m}$
One-to-one	$1220 \pm 337 \text{ nm}$
One-to-one + DFS + WFS	$904 \pm 145 \text{ nm}$
One-to-one + DFS + WFS + knobs	$58.4 \pm 4.7 \text{ nm}$

Intensity-dependent effects in ATF2 Simulations

Impact of static errors

Impact of static errors in ATF2: Simulation conditions

Simulated errors:

- Static errors:
 - Misalignment of quadrupoles, sextupoles, BPMs of 100 μm RMS.
 - Strength error of quadrupoles, sextupoles of 0.01% RMS.
 - Roll error for quadrupoles and sextupoles of 200 μrad RMS.

Corrections applied:

- One-to-one
- DFS
- WFS
- Knobs (Y, YP D XP XP.*XP XP.*YP XP.*D)


Simulation procedure:

- 100 machines with the previously cited static imperfections.
- Apply the cited corrections and the knobs on the distribution at the IP.
- Each simulation set will study the impact of a specific static error.

Tracking code used: PLACET

Impact of static errors in ATF2: Misalignment

Misalignment of quadrupoles, sextupoles, BPMs of 100 μm RMS:

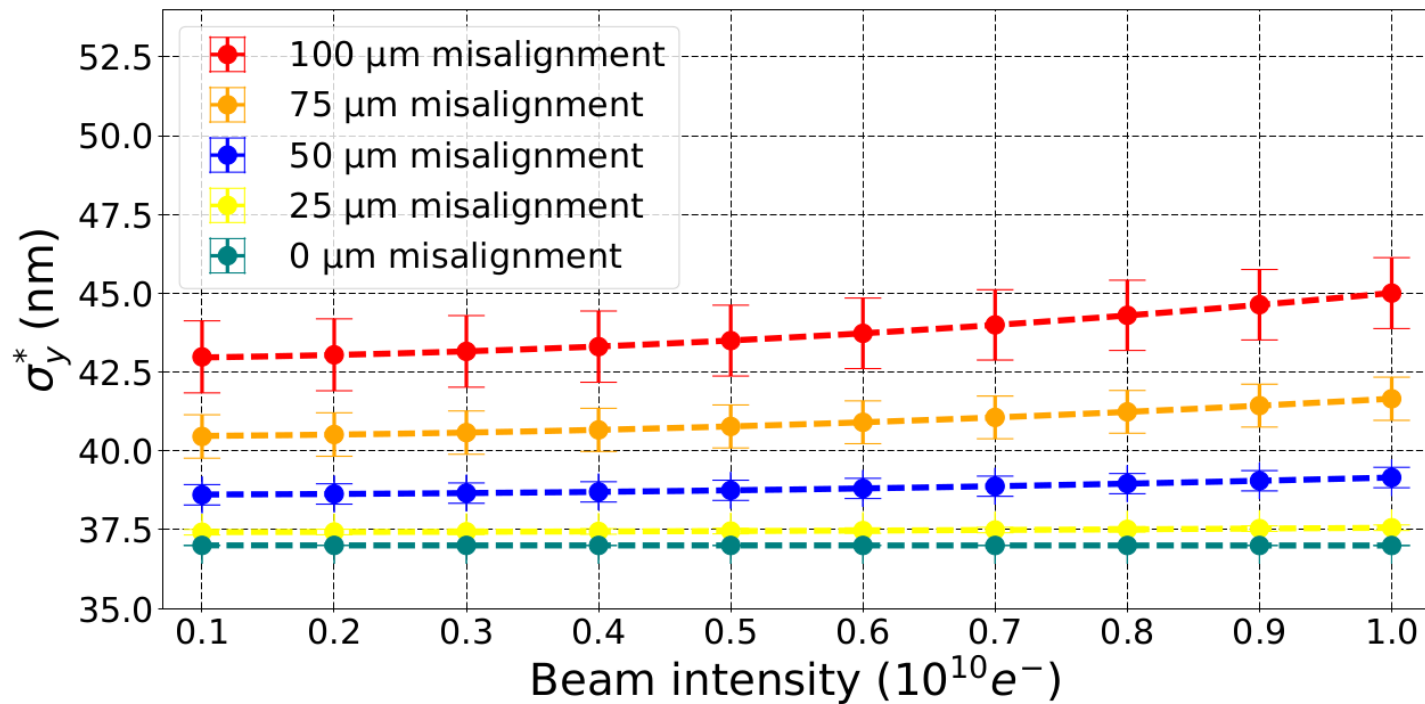


Figure: Effect of the misalignments on the vertical beam size at the IP (σ_y^*) vs. the beam intensity with wakefields calculated with PLACET.

Impact of static errors in ATF2: Strength error

Strength error of quadrupoles, sextupoles of 0.01% (+ misalignment 100 μm):

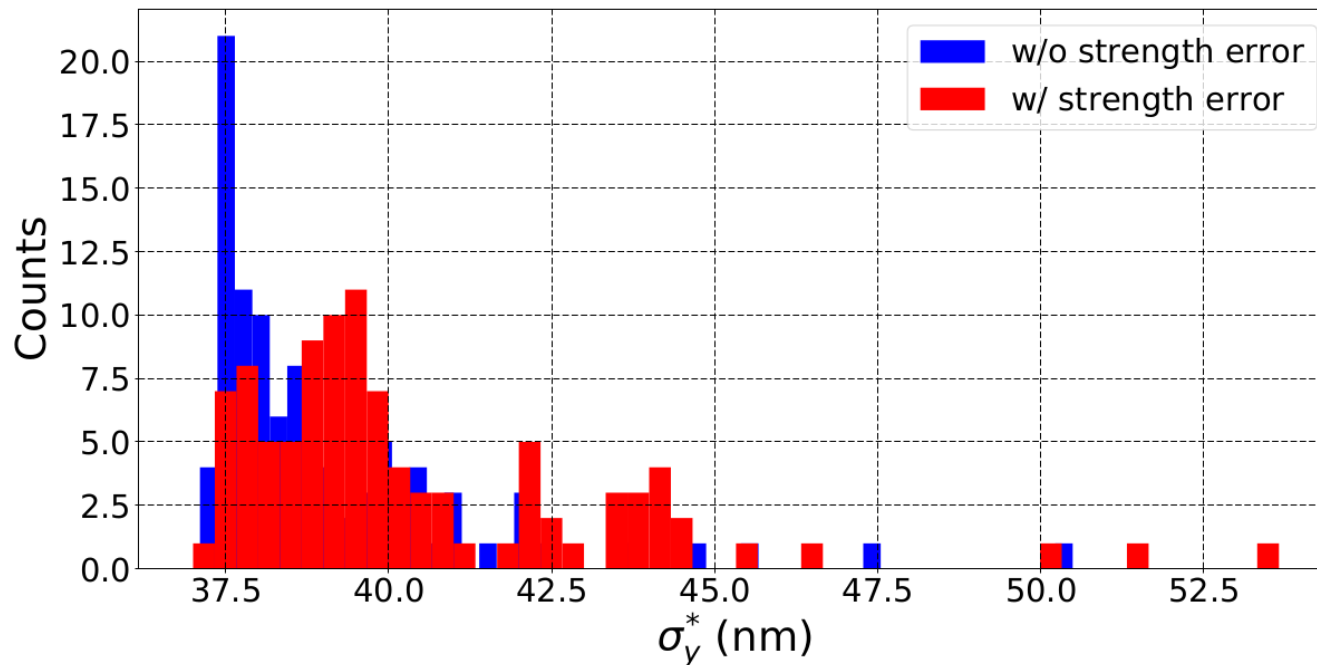


Figure : Effect of quadrupoles and sextupoles strength error of 10^{-4} RMS at $1.0 \times 10^{10} e^-$ on the vertical IP beam size (σ_y^*), in presence of wakefields calculated with PLACET.

Impact of static errors in ATF2: Roll error

Roll error for quadrupoles and sextupoles of 200 μrad :

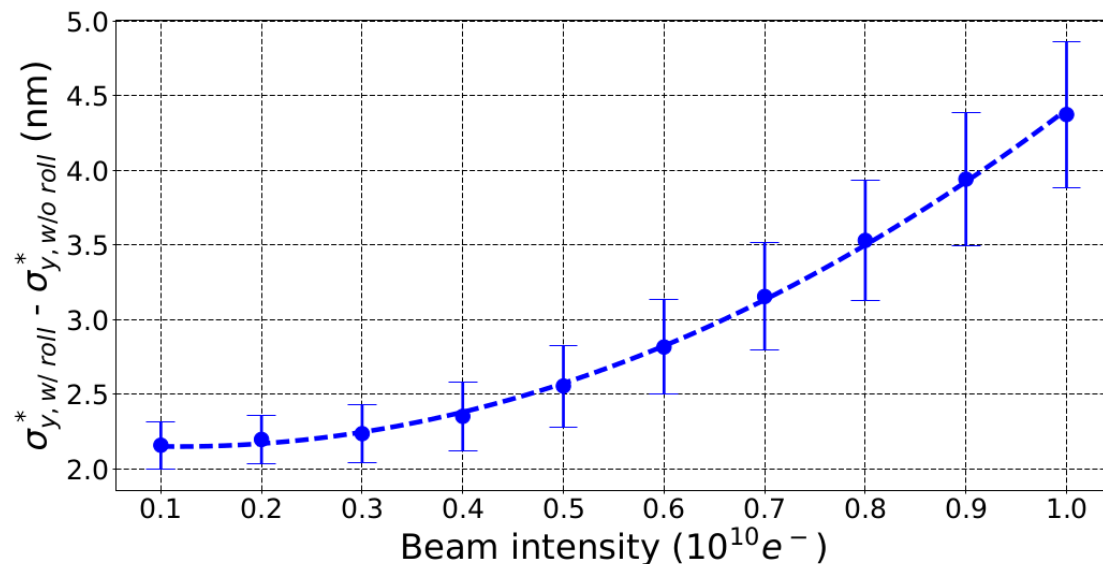


Figure: Effect of 200 μrad RMS rolls of BPMs, quadrupoles and sextupoles on the vertical IP beam size (σ_y^*) vs. the beam intensity, in presence of wakefields calculated with PLACET.

Static error	Misalignment	Strength error	Roll error
Error amplitude	100 [μm]	1×10^{-4}	200 [μrad]
Average σ_y^* at $10^9 e^-$ [nm]	43 ± 1.1	39 ± 0.09	39 ± 0.16
Average σ_y^* at $10^{10} e^-$ [nm]	45 ± 1.1	42 ± 0.29	41 ± 0.49

Intensity-dependent effects in ATF2 Simulations

Impact of dynamic errors

Impact of dynamic errors in ATF2: Simulation conditions

Simulated errors:

Static errors:

- Misalignment of quadrupoles, sextupoles and BPMs of 100 μm RMS.
- Strength error of quadrupoles and sextupoles of 0.1% RMS.
- Roll error for quadrupoles and sextupoles of 200 μrad RMS.

Dynamic errors:

- Incoming pos. & ang. jitter of $[0.1\sigma_y - 1.0\sigma_y]$

Corrections applied:

- One-to-one
 - DFS
 - WFS
 - Knobs (Y, YP D XP XP.*XP XP.*YP XP.*D)
- 

Simulation procedure:

Tracking 200 bunches per machine from the ATF extraction line to the IP.

100 machines with the previously cited static imperfections.

Apply the cited corrections and the knobs on the distribution at the IP.

Impact of dynamic errors in ATF2: Incoming position jitter

Incoming position jitter of $[0.1\sigma_y - 0.5\sigma_y]$:

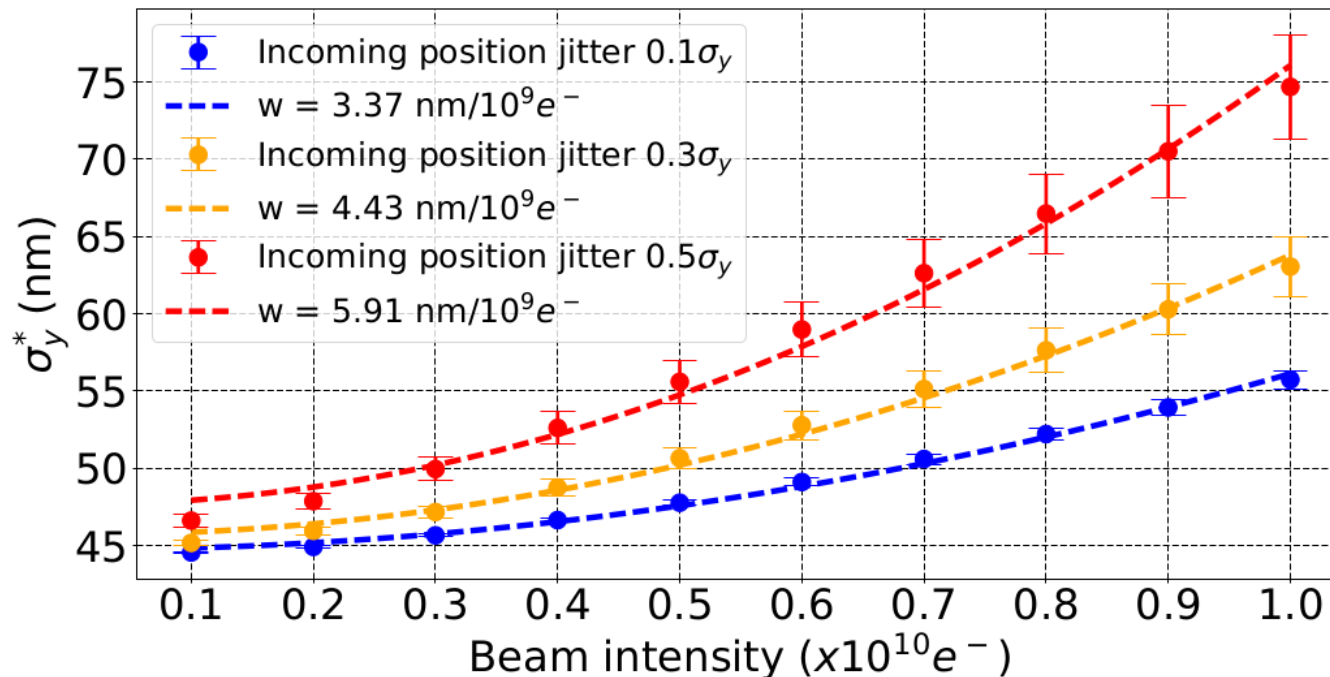


Figure: Effect of incoming 0.1, 0.3 and 0.5 σ_y beam position jitter on the vertical beam size at the IP (σ_y^*) vs. the beam intensity, calculated with PLACET in presence of wakefields.

$$w [nm/10^9] = (\sqrt{\sigma_{y,q}^2 - \sigma_{y,0}^2})/q$$

Impact of dynamic errors in ATF2: Incoming angle jitter

Incoming angle jitter of $[0.1\sigma_{y'}, -0.5\sigma_{y}']$:

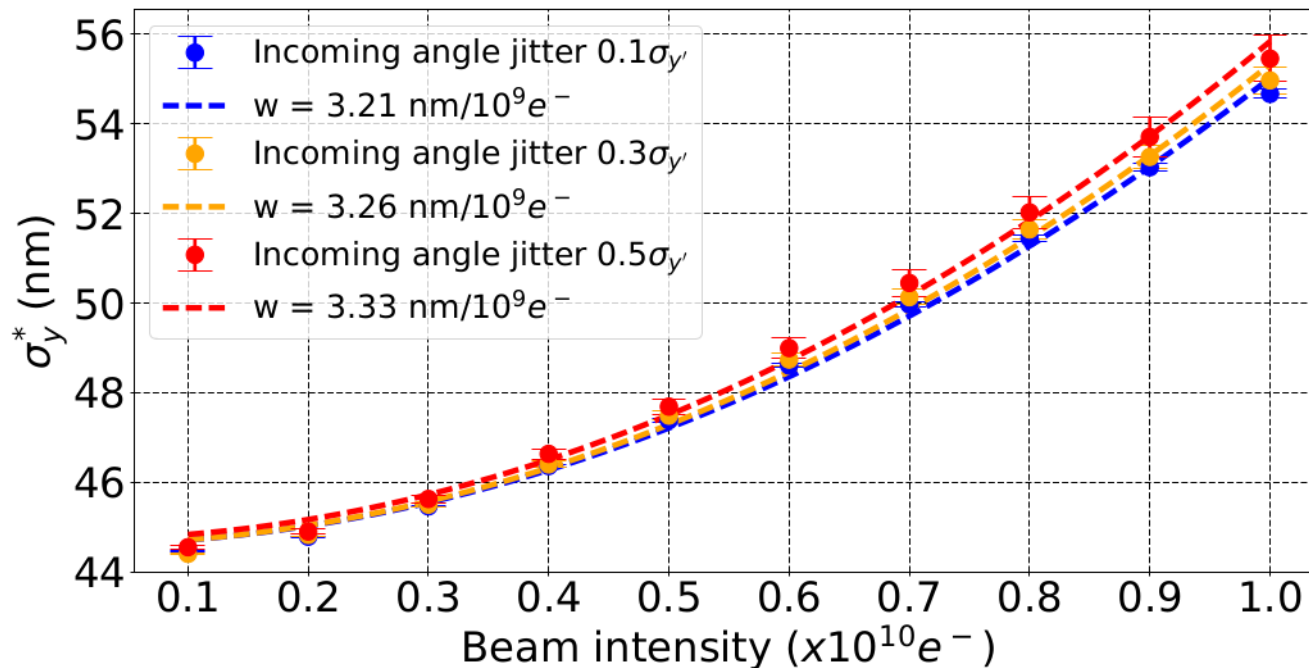


Figure: Effect of incoming 0.1, 0.3 and 0.5 $\sigma_{y'}$ beam angle jitter on the vertical beam size at the IP (σ_y^*) vs. the beam intensity, calculated with PLACET in presence of wakefields.

$$w [nm/10^9] = (\sqrt{\sigma_{y,q}^2 - \sigma_{y,0}^2})/q$$

Impact of dynamic errors in ATF2: Incoming position and angle jitter

Incoming position and angle jitter of $[0.1\sigma_{y'}, -1.0\sigma_{y'}]$:

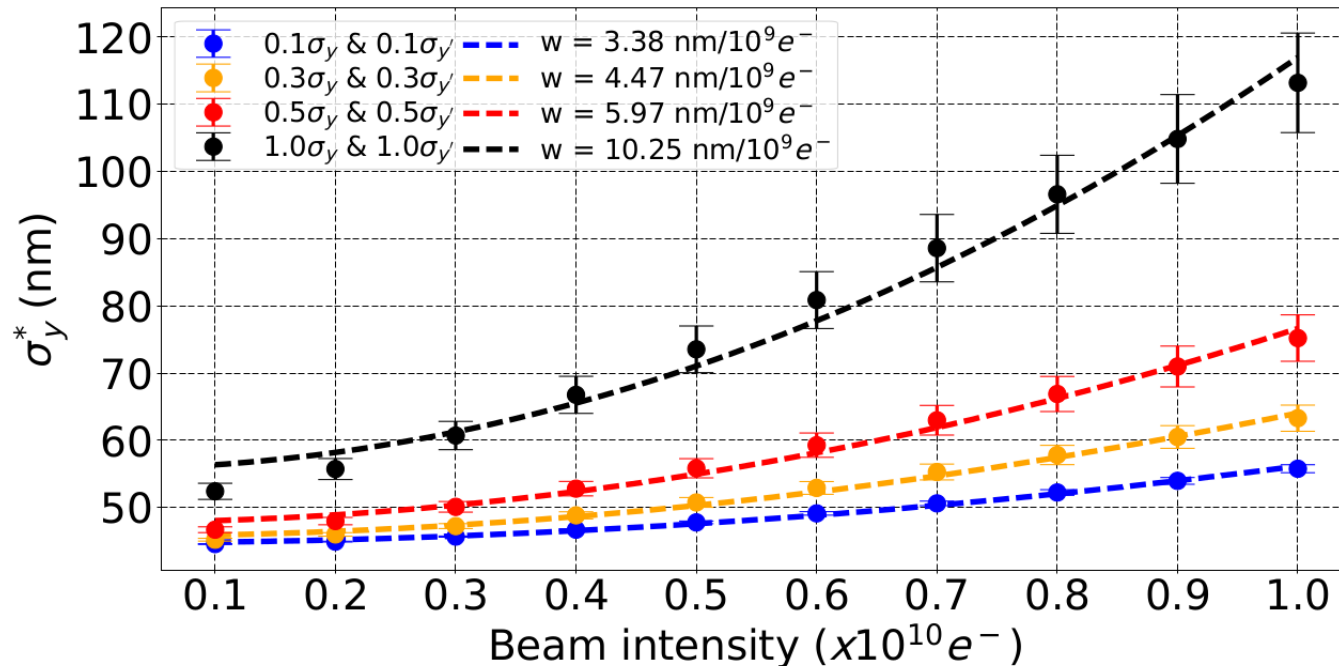


Figure: Effect of both incoming $0.1, 0.3, 0.5$ and $1.0 \sigma_y$ beam position and $0.1, 0.3, 0.5$ and $1.0 \sigma_{y'}$ beam angle jitters on the vertical beam size at the IP (σ_y^*) vs. the beam intensity, calculated with PLACET in presence of wakefields.

$$w [nm/10^9] = (\sqrt{\sigma_{y,q}^2 - \sigma_{y,0}^2}) / q$$

Impact of dynamic errors in ATF2: Incoming position and angle jitter summary

Jitter	w [nm/10⁹ e⁻]	Intensity [e⁻]	Average σ_y^* [nm]
Inc. position jitter $0.1\sigma_y$ and angle jitter $0.1\sigma_{y'}$	3.38	1.0×10^9 10.0×10^9	45 ± 0.05 56 ± 0.59
Inc. position jitter $0.3\sigma_y$ and angle jitter $0.3\sigma_{y'}$	4.47	1.0×10^9 10.0×10^9	45 ± 0.20 63 ± 1.95
Inc. position jitter $0.5\sigma_y$ and angle jitter $0.5\sigma_{y'}$	5.97	1.0×10^9 10.0×10^9	47 ± 0.42 75 ± 3.45
Inc. position jitter $1.0\sigma_y$ and angle jitter $1.0\sigma_{y'}$	10.25	1.0×10^9 10.0×10^9	52 ± 1.20 113 ± 7.41

Static error	Misalignment	Strength error	Roll error
Error amplitude	100 [μm]	1×10^{-4}	200 [μrad]
σ_y^* growth at $10^9 e^-$	16%	4%	6%
σ_y^* growth at $10^{10} e^-$	22%	15%	12%
Dynamic error	Angle jitter	Position jitter	Both jitters
Error amplitude	$0.5\sigma_{y'}$	$0.5\sigma_y$	$0.5\sigma_y$ and $0.5\sigma_{y'}$
σ_y^* growth at $10^9 e^-$	22%	27%	27%
σ_y^* growth at $10^{10} e^-$	49%	103%	103%

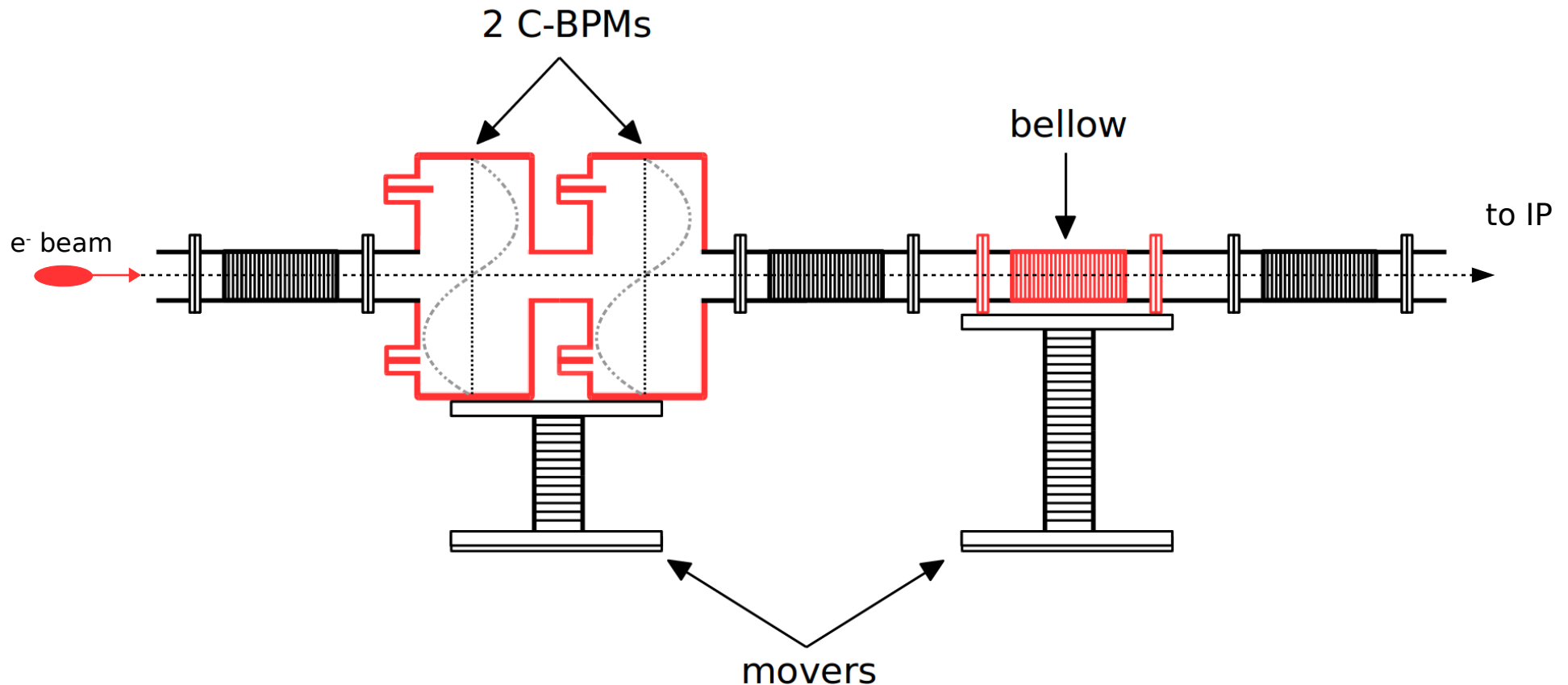
Intensity-dependent effects in ATF2 Simulations

Wakefield knobs

Wakefield knobs Experimental setup (1/2)

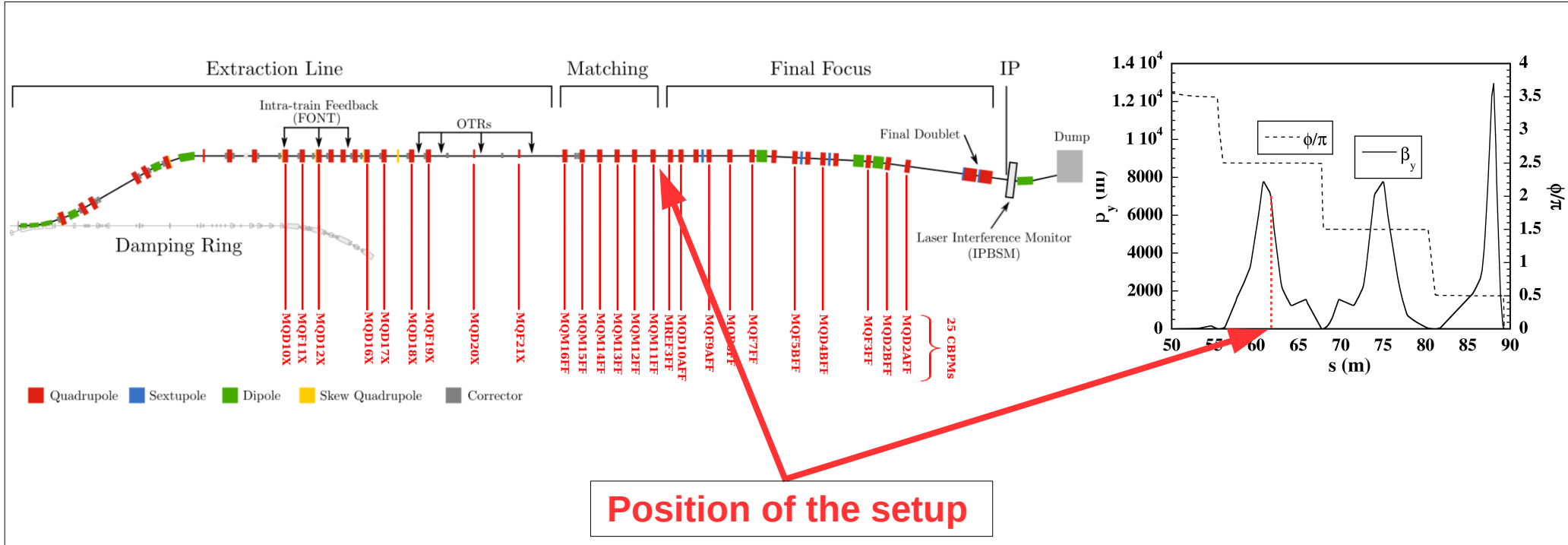
Goal: Use two well known wakefield sources on movers in the ATF2 extraction line to compensate the intensity-dependent effects.

Setup: Made of two movers, the first one carries two C-BPMs and the second one carries a bellows.



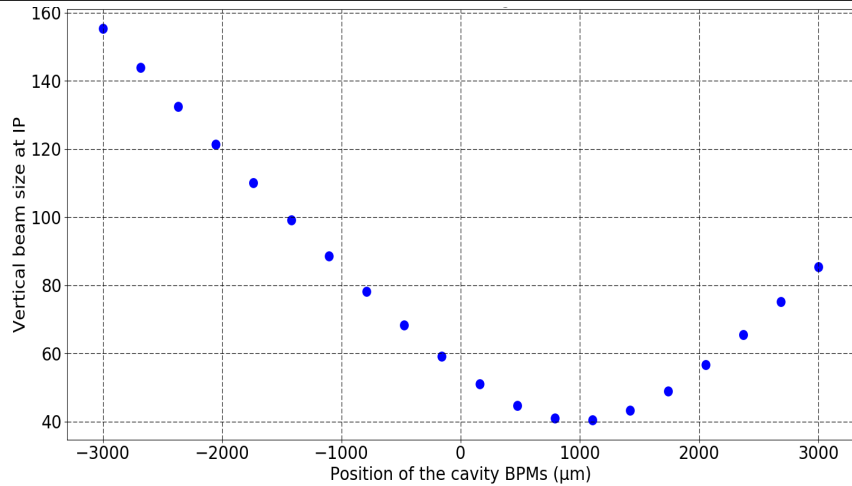
Wakefield knobs Experimental setup (2/2)

Position: The setup was installed in the the ATF2 extraction line between QD10BFF and QD10AFF. The phase between the setup and the IP is around 2.5π . Thus, the kicks generated by the setup translate into a position offset at IP.

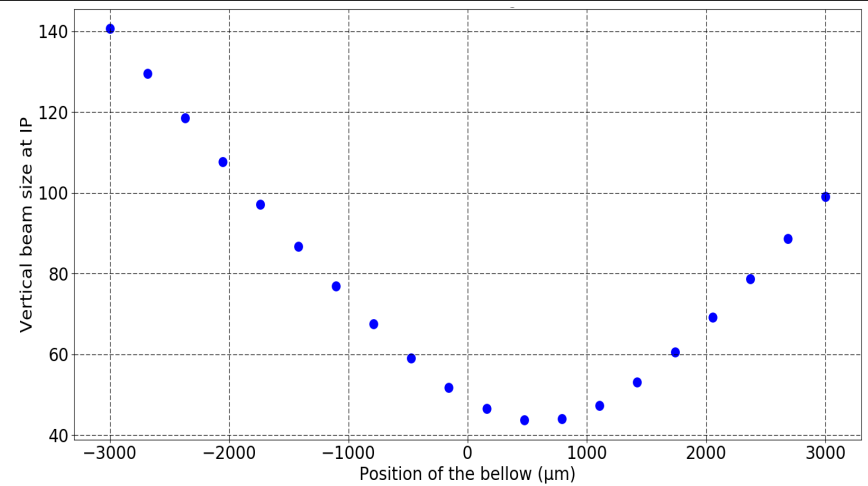


Wakefield knobs Simulations (1/2)

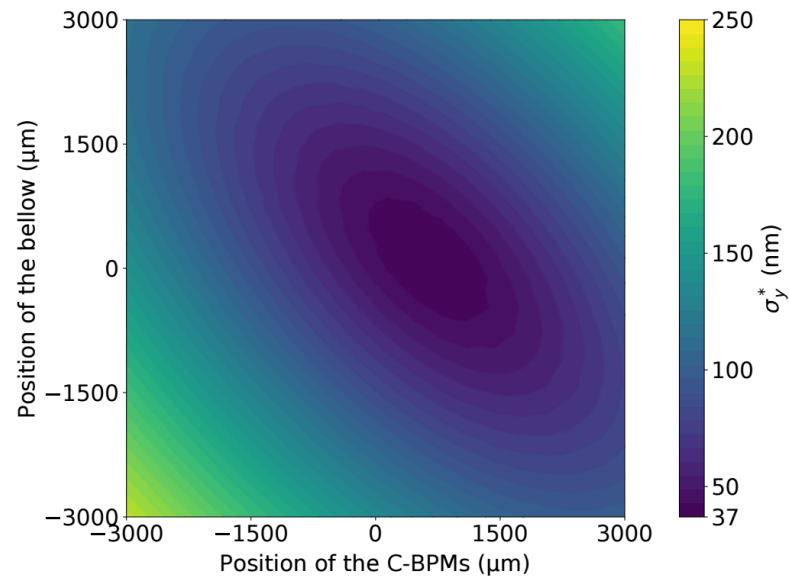
Position of CBPMs scan for one machine.



Position of bellows scan for one machine.



2D scan for
one machine



Wakefield knobs Simulations (2/2)

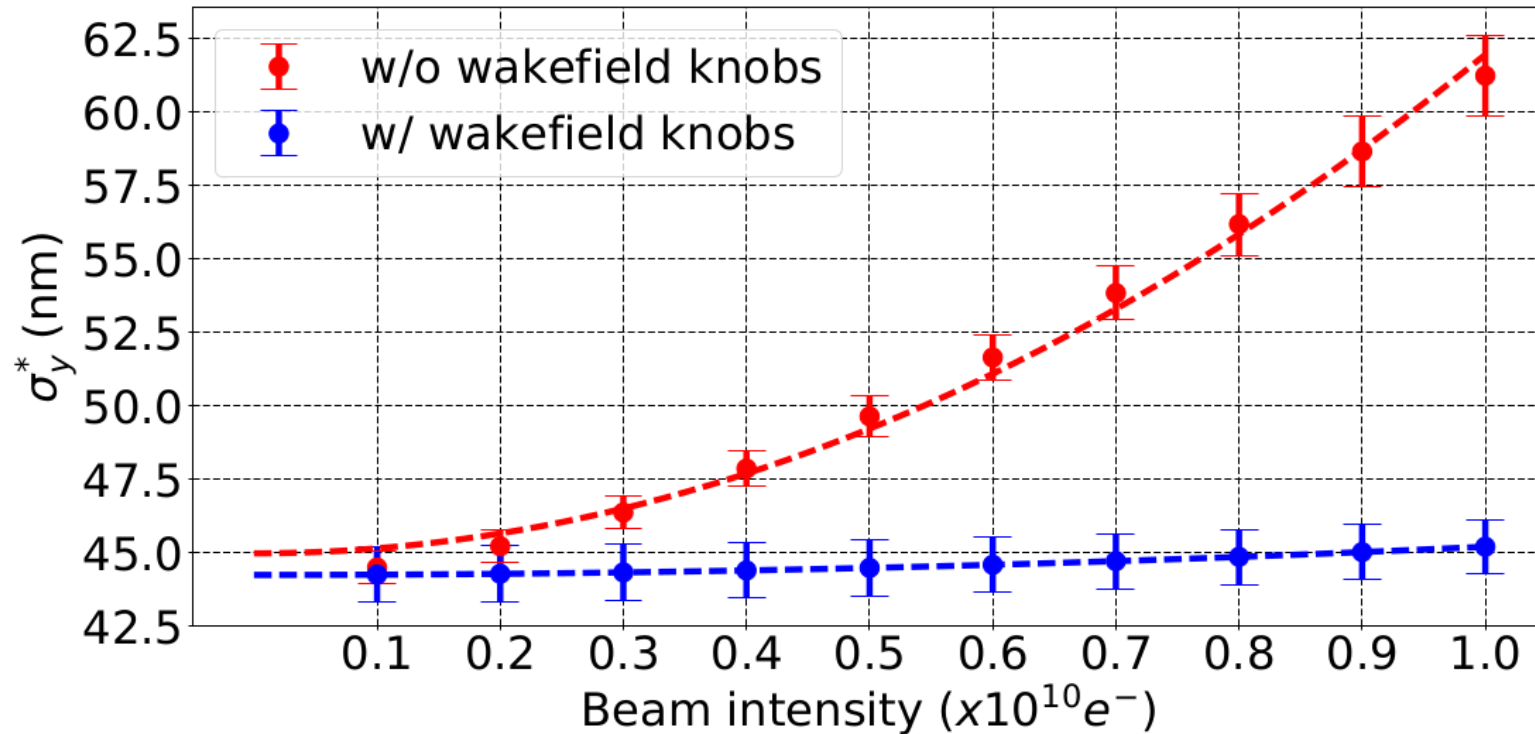


Figure: Simulations of the impact of the ATF2 wakefield knobs on the vertical IP beam size (σ_y^*).

Case	$\overline{\sigma_y^*}$ [nm]
No source on movers	61.2 ± 1.4
Using the bellow on mover	48.4 ± 1.0
Using the 2 C-BPMS on mover	45.5 ± 0.9
Using both the bellow and the 2 C-BPMs on movers	45.2 ± 0.9

Intensity-dependent effects in ATF2 Measurements

Impact of corrections

The IP Beam Size Monitor or Shintake Monitor

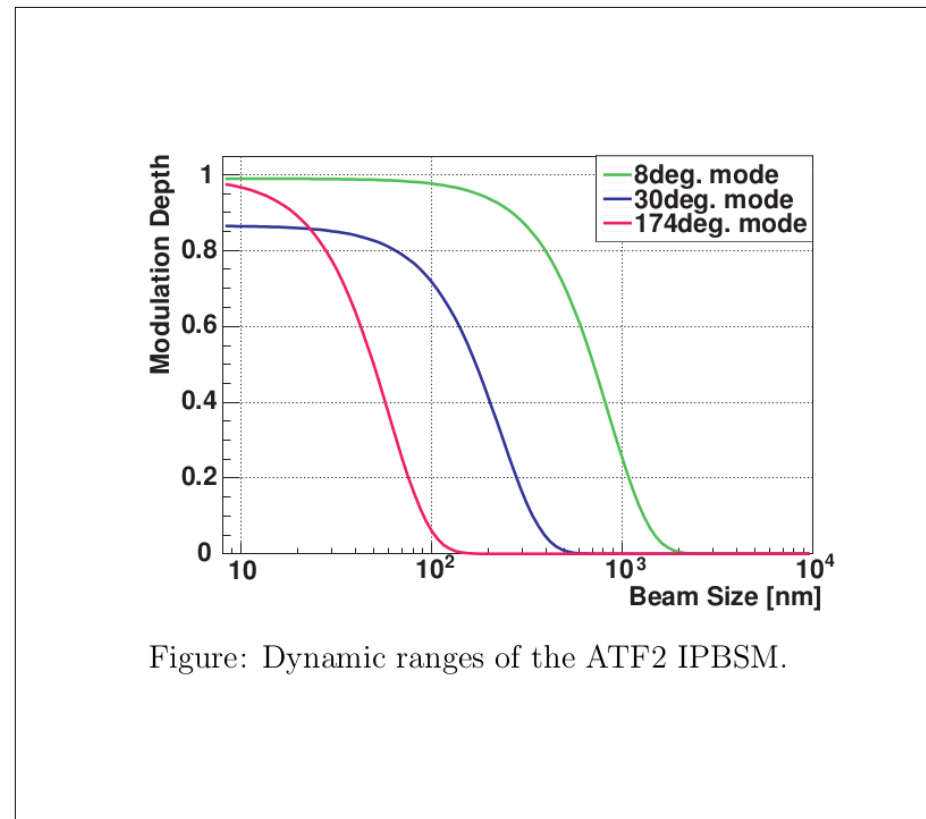
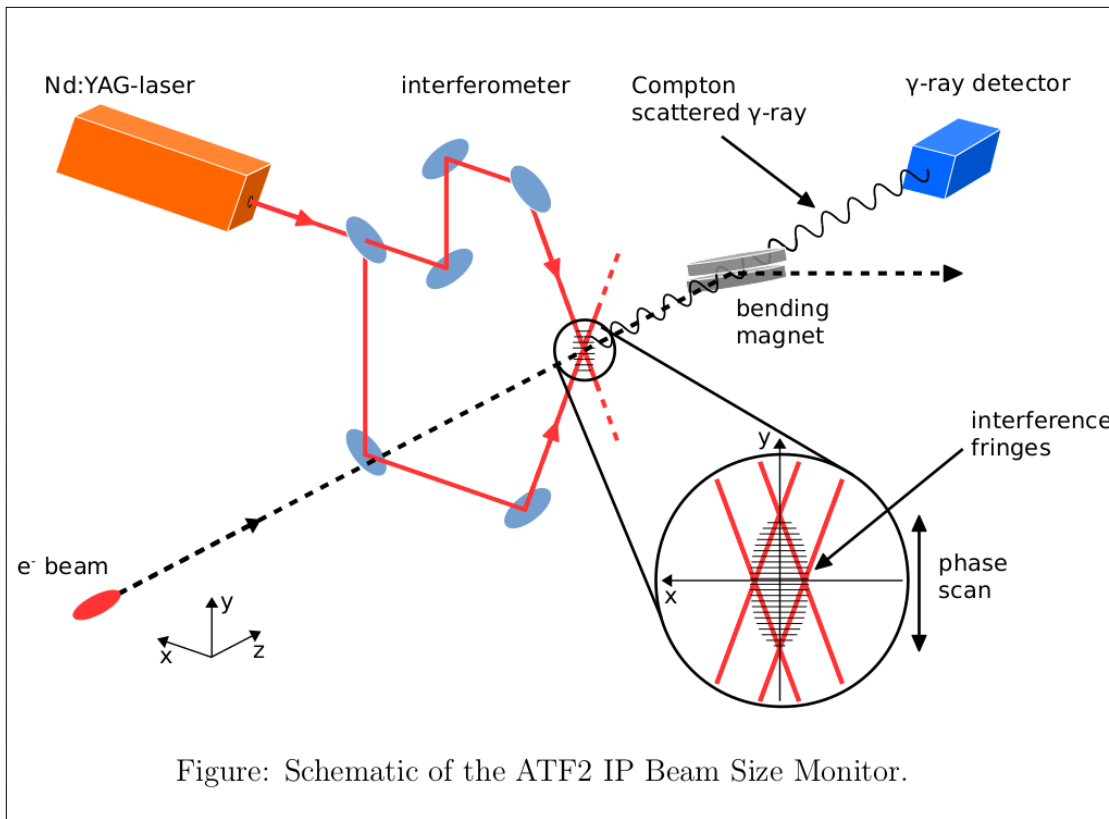


Table: Dynamic range of the IPBSM.

Crossing angle θ	174°	30°	2-8°
Measurable σ_y^*	25 - 100 nm	80 - 400 nm	360 nm - 6 μm

$$\sigma_y = \frac{1}{C} \sqrt{\frac{1}{2} \ln \left(\frac{C |\cos \theta|}{M} \right)}$$

Dispersion Free Steering Experimental results

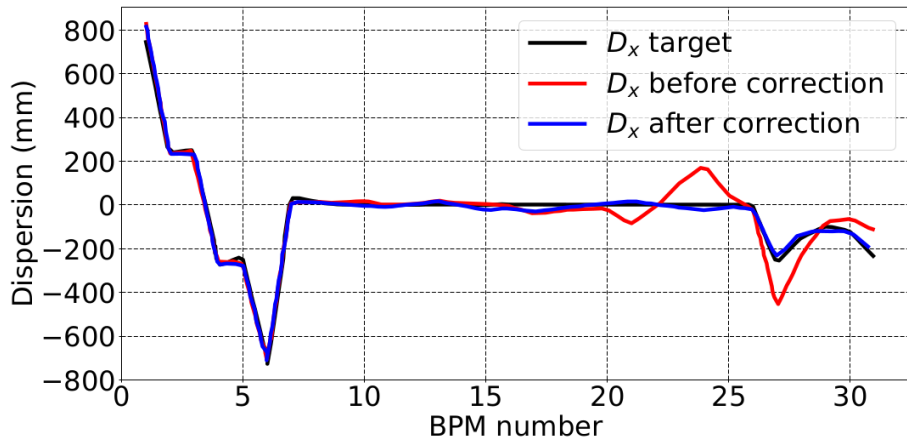
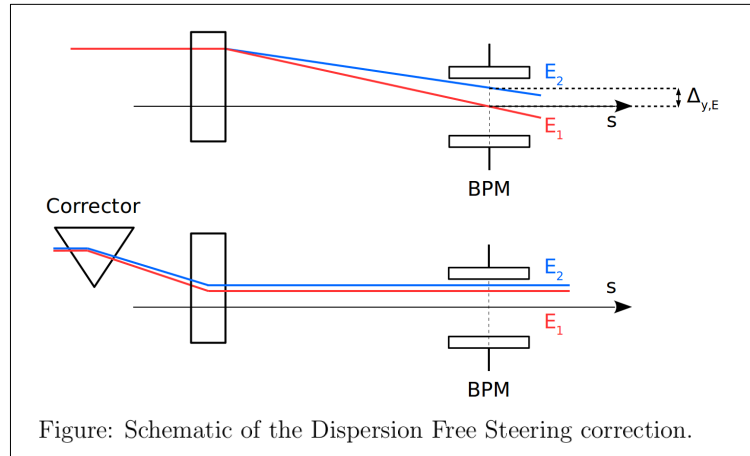


Figure: Measured horizontal dispersion (D_x) in the ATF2 beamline before and after applying DFS correction vs. BPM number.

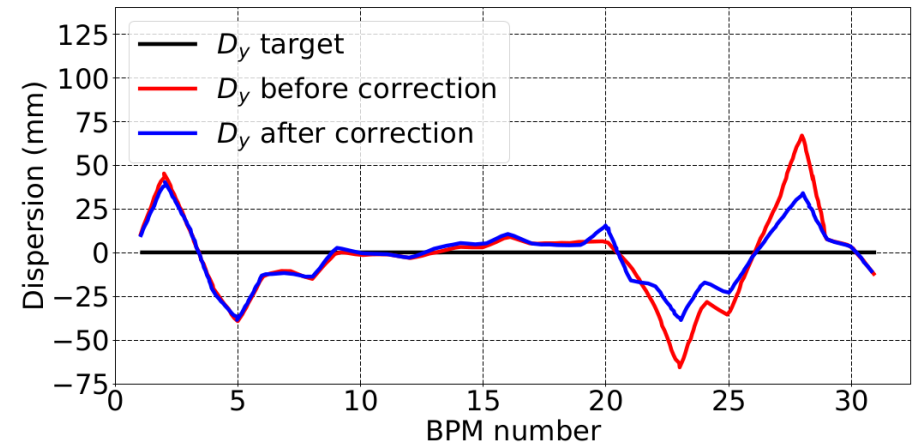


Figure: Measured vertical dispersion (D_y) in the ATF2 beam line before and after DFS correction vs. BPM number.

Wakefield Free Steering Experimental results

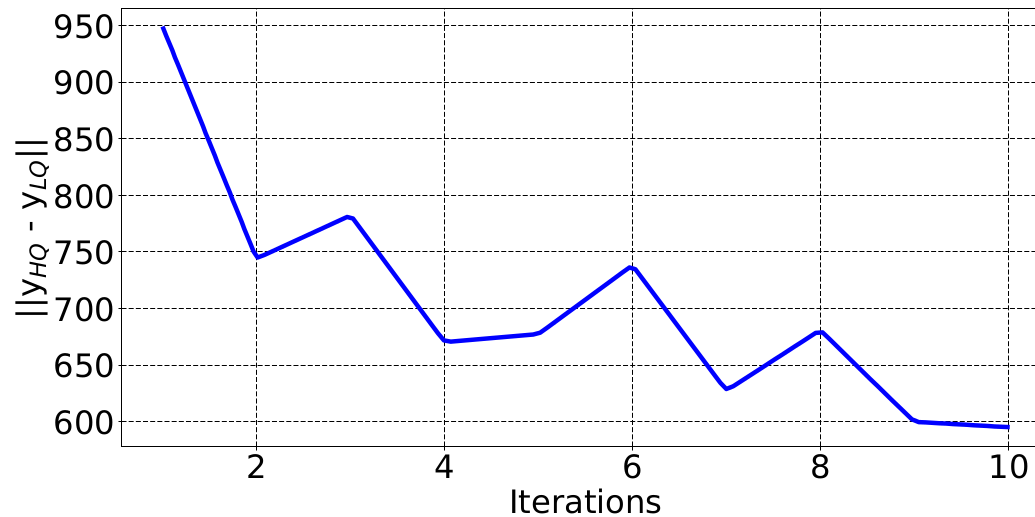
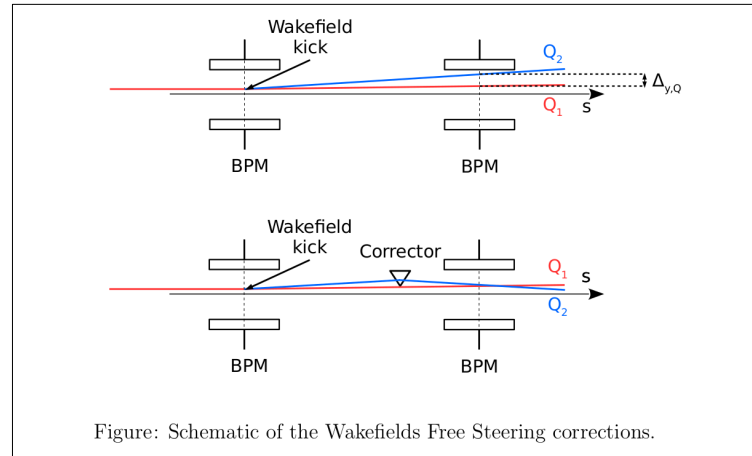


Figure: Measurement: impact of Wakefield Free Steering on the vertical orbit.

$$\|y_{HQ} - y_{LQ}\| = \sqrt{\sum |y_{HQ} - y_{LQ}|^2}$$

Dispersion Free Steering and Wakefield Free Steering Experimental results

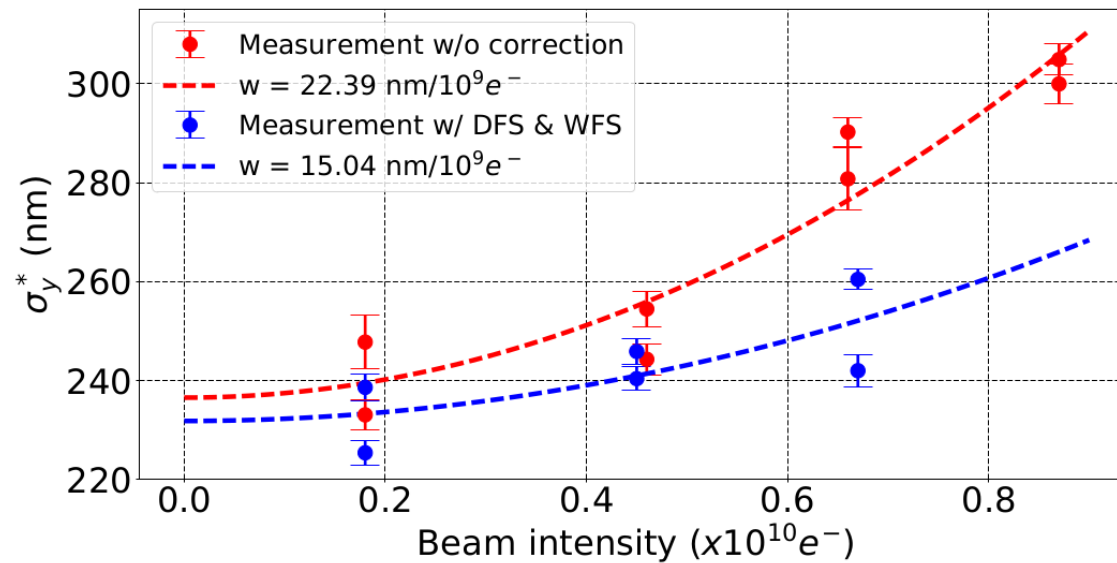
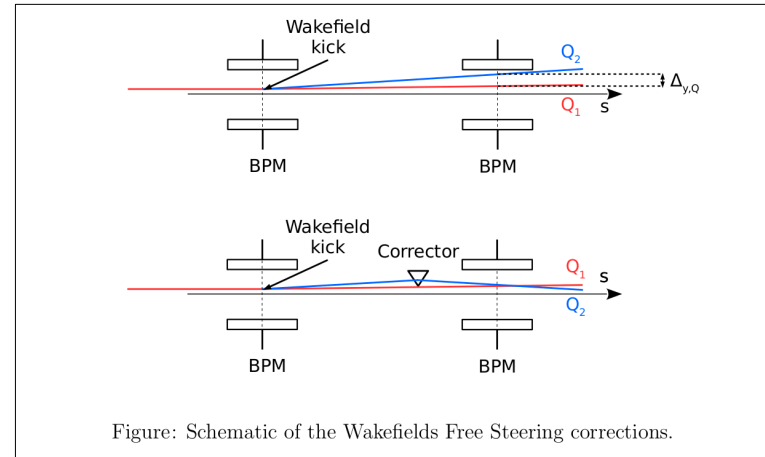
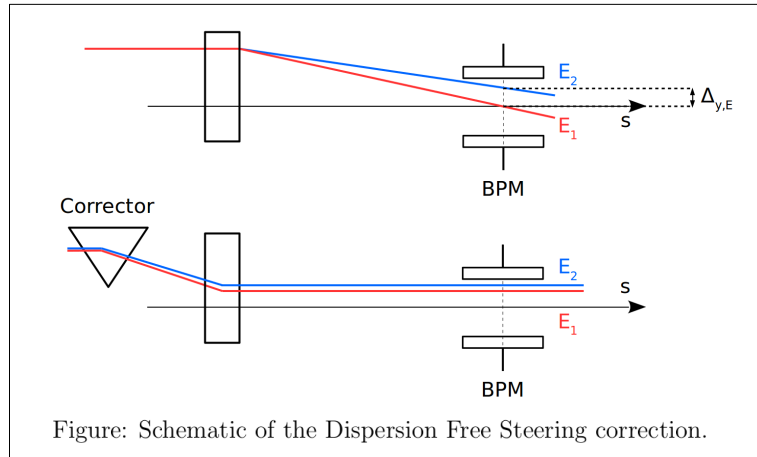


Figure: Measurement: impact of DFS and WFS on the vertical beam size at the IP.

Wakefield knobs Experimental results*

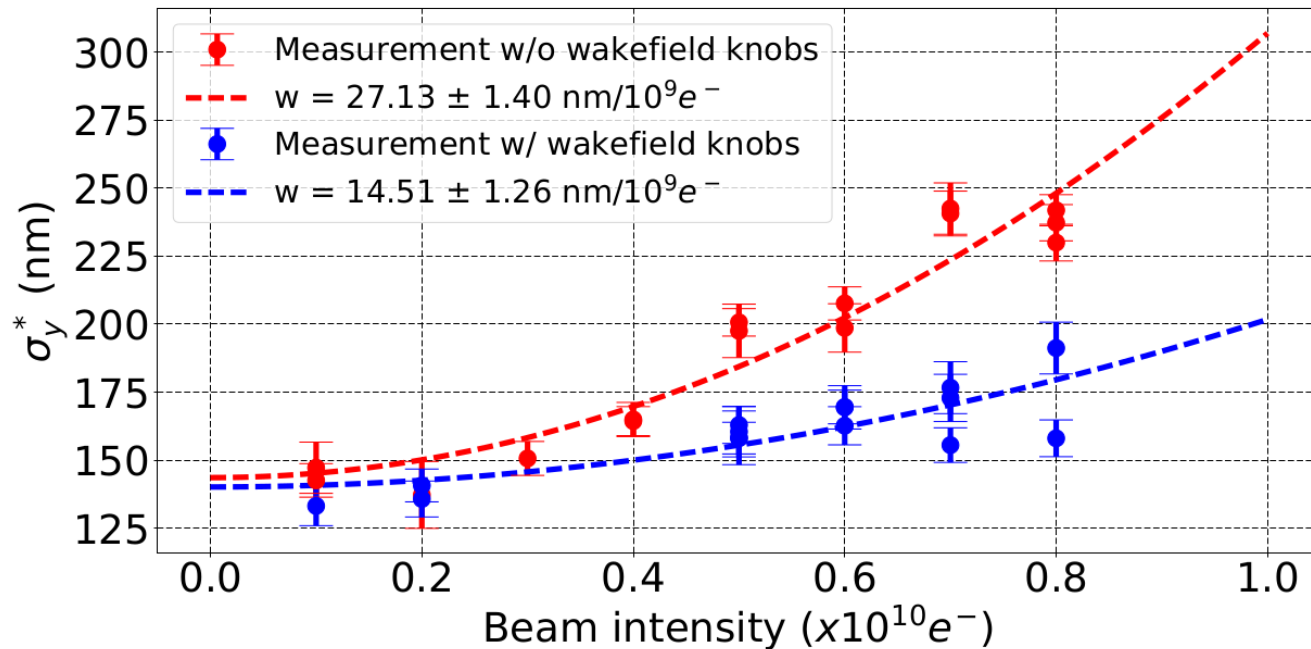


Figure : Measured vertical IP beam size (σ_y^*) vs. the beam intensity before and after applying wakefield knobs.

$$w [nm/10^9] = (\sqrt{\sigma_{y,q}^2 - \sigma_{y,0}^2})/q$$

*Using the IPBSM 30° mode

The wakefield knobs reduced the intensity dependence parameter from **27.13 nm/10⁹** to **14.51 nm/10⁹**. (The IP angle jitter was **70 urad**).

Intensity-dependent effects in ATF2 Measurements

Comparison simulations/measurements

Comparison intensity-dependent effects Simulations/Measurements

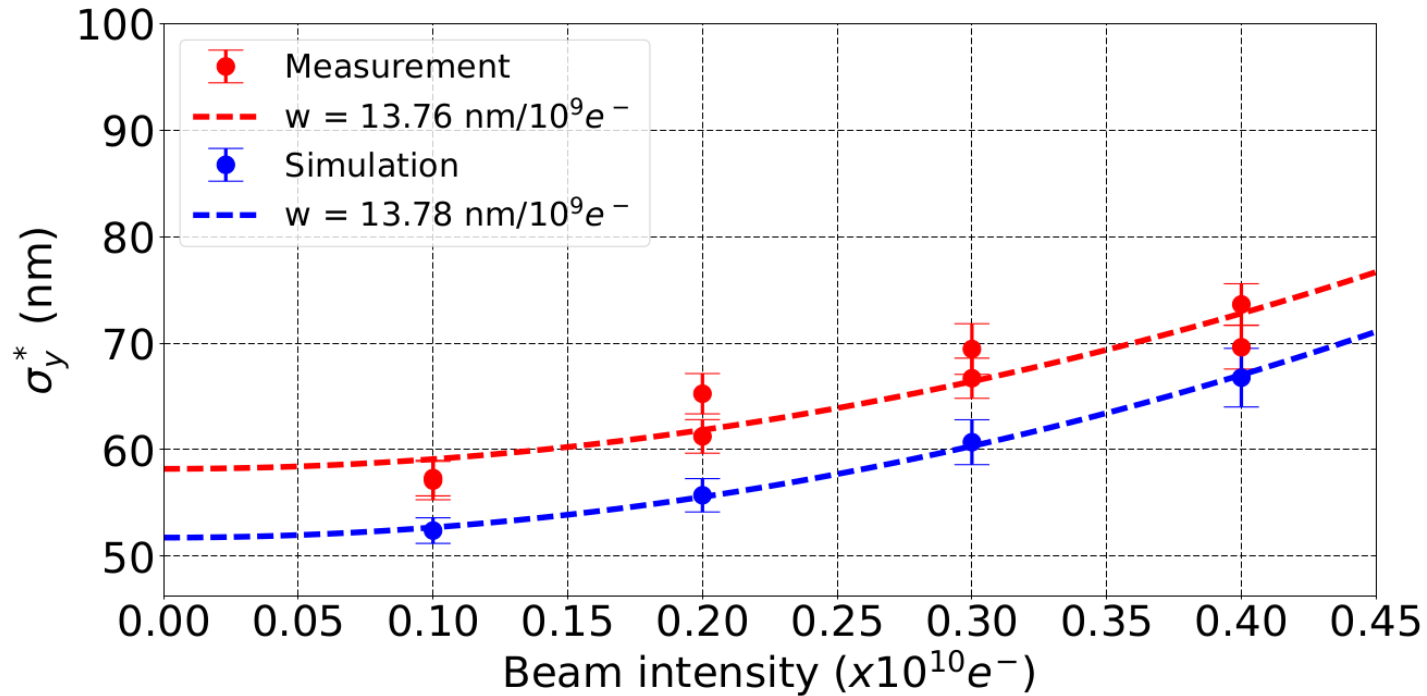


Figure: Comparison between measurements and simulations of the vertical beam size at the IP (σ_y^*) vs. the beam intensity and the intensity-dependent parameter w .

Case	w [nm/10 ⁹ e ⁻]	Beam intensity [e ⁻]	Average σ_y^* [nm]
Measurement	13.76	0.1 × 10 ¹⁰	57 ± 1.7
		0.2 × 10 ¹⁰	63 ± 1.7
		0.3 × 10 ¹⁰	68 ± 2.1
		0.4 × 10 ¹⁰	72 ± 2.0
Simulation	13.78	0.1 × 10 ¹⁰	52 ± 1.2
		0.2 × 10 ¹⁰	56 ± 1.6
		0.3 × 10 ¹⁰	61 ± 2.1
		0.4 × 10 ¹⁰	67 ± 2.8

Impact of short-range and long-range wakefields in the 380 GeV CLIC BDS

Introduction

The Compact Linear Collider

The Compact Linear Collider is an electron/positron head-on collider at energies of up to 3 TeV. For an optimal exploitation of its physics potential, CLIC is intended to be built and operated in three stages, at collision energies of 380 GeV, 1.5 TeV and 3 TeV respectively, for a site length ranging from 11 to 50 km. The physics aims of CLIC include high-precision measurements of the Higgs boson's interactions with other particles and with itself.

The latest information and parameters can be found in the CLIC Project Implementation Plan [10] (2018).

CERN-2018-010-M
20 December 2018

ORGANISATION EUROPÉENNE POUR LA RECHERCHE NUCLÉAIRE
CERN EUROPEAN ORGANIZATION FOR NUCLEAR RESEARCH



THE COMPACT LINEAR COLLIDER (CLIC)
PROJECT IMPLEMENTATION PLAN

GENEVA
2018

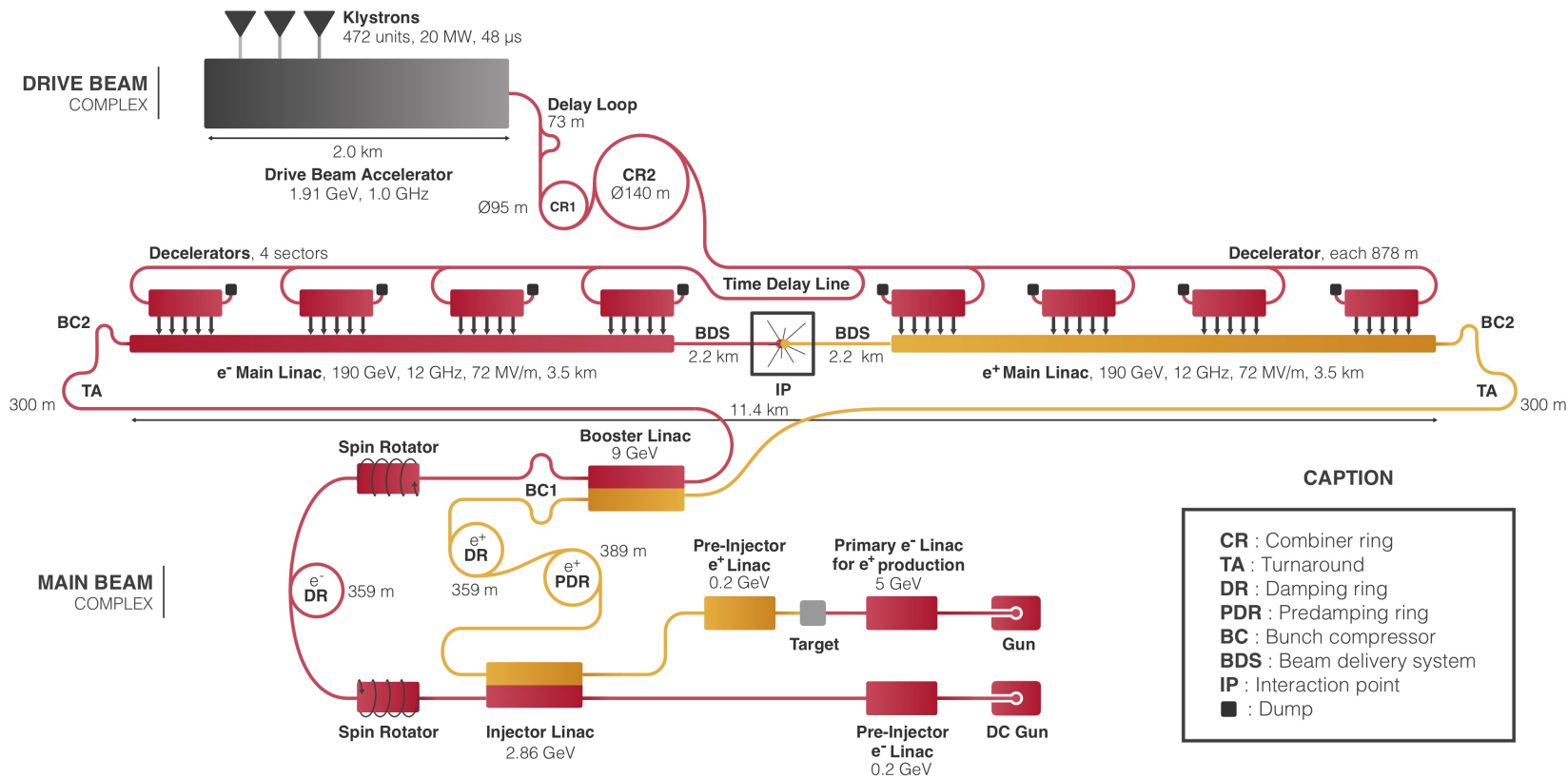
Table: Key parameters of 380 GeV baseline collider.

Parameter	Symbol	Unit	
Centre-of-mass energy	\sqrt{s}	GeV	380
Repetition frequency	f_{rep}	Hz	50
Number of bunches per train	n_b		352
Bunch separation	Δt	ns	0.5
Pulse length	τ_{RF}	ns	244
Accelerating gradient	G	MV/m	72
Total luminosity	\mathcal{L}	$10^{34} \text{ cm}^{-2}\text{s}^{-1}$	1.5
Luminosity above 99% of \sqrt{s}	$\mathcal{L}_{0.01}$	$10^{34} \text{ cm}^{-2}\text{s}^{-1}$	0.9
Main tunnel length		km	11.4
Number of particles per bunch	N	10^9	5.2
Bunch length	σ_z	μm	70
IP beam size	σ_x/σ_y	nm	149/2.9
Normalised emittance (end of linac)	ϵ_x/ϵ_y	nm	900/20

Introduction

The Compact Linear Collider

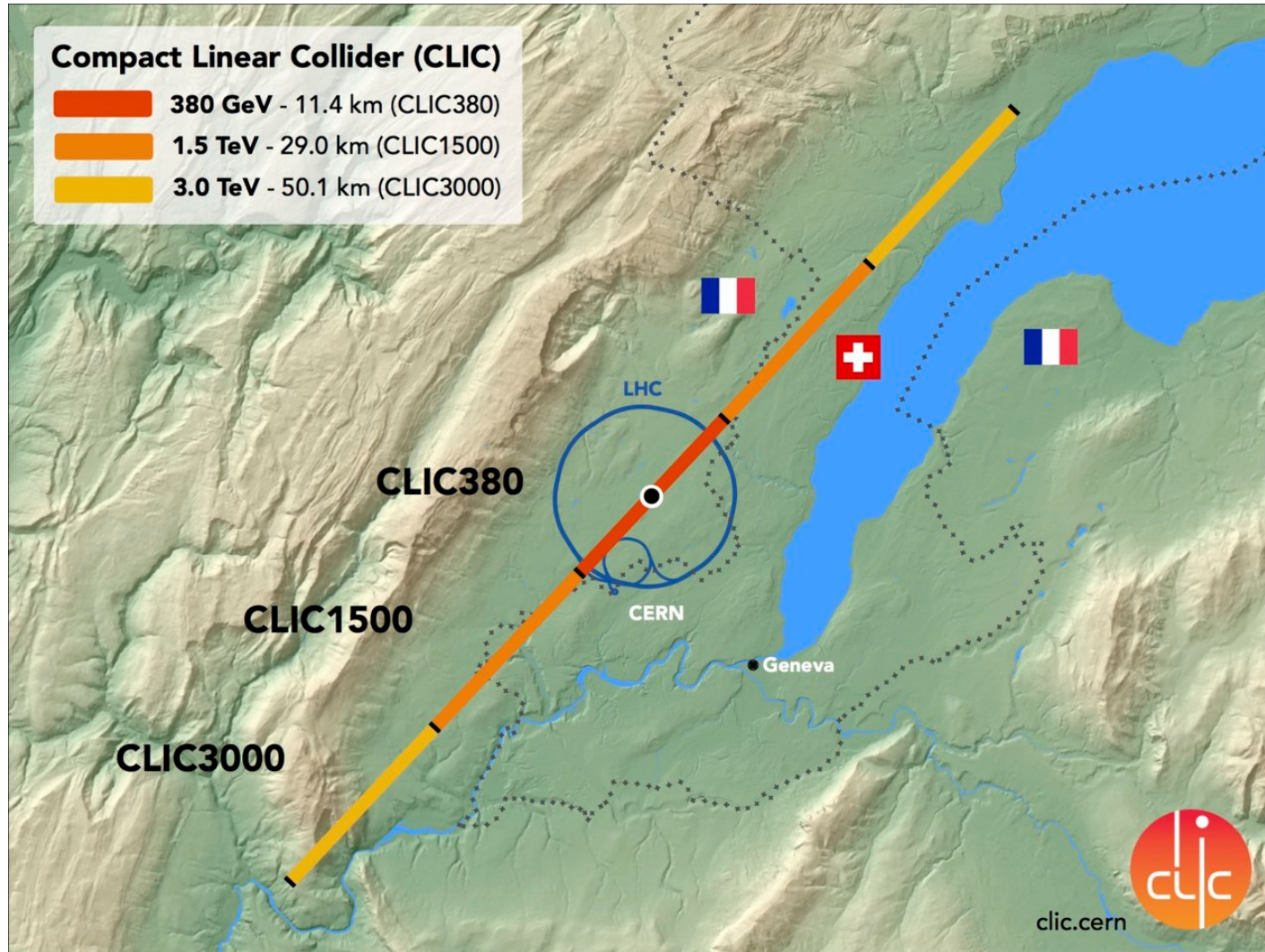
CLIC would use a novel scheme, the two-beam-acceleration. The so-called **Drive Beam** would run parallel to the colliding Main Beam. The Drive Beam is decelerated in special devices called Power Extraction and Transfer Structures (PETS) that extract energy from the Drive Beam in the form of powerful Radio Frequency (RF) waves, which is then used to accelerate the Main Beam. Up to 90% of the energy of the Drive Beam is extracted and efficiently transferred to the Main Beam.



380 GeV

Introduction

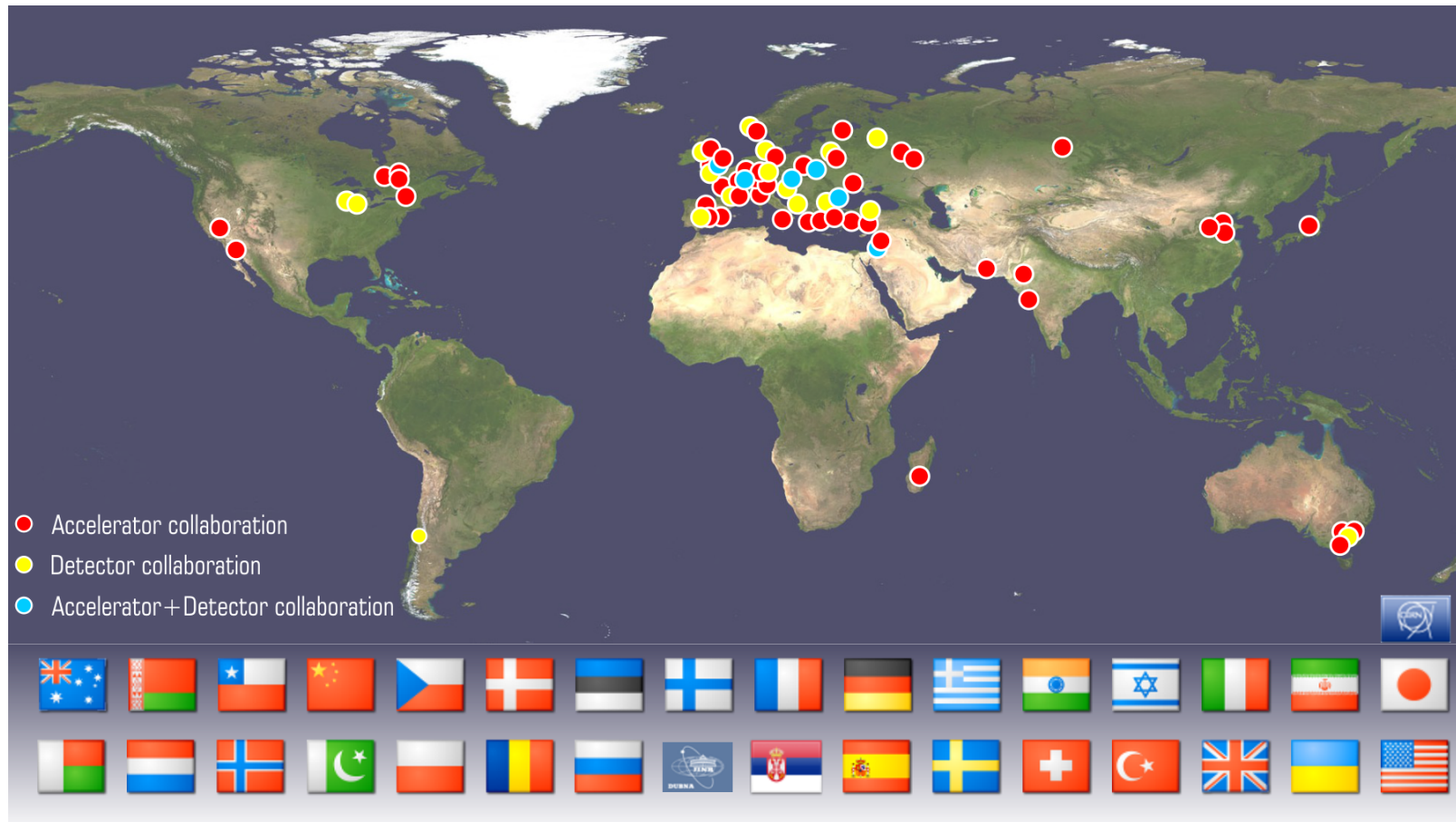
The Compact Linear Collider



Introduction

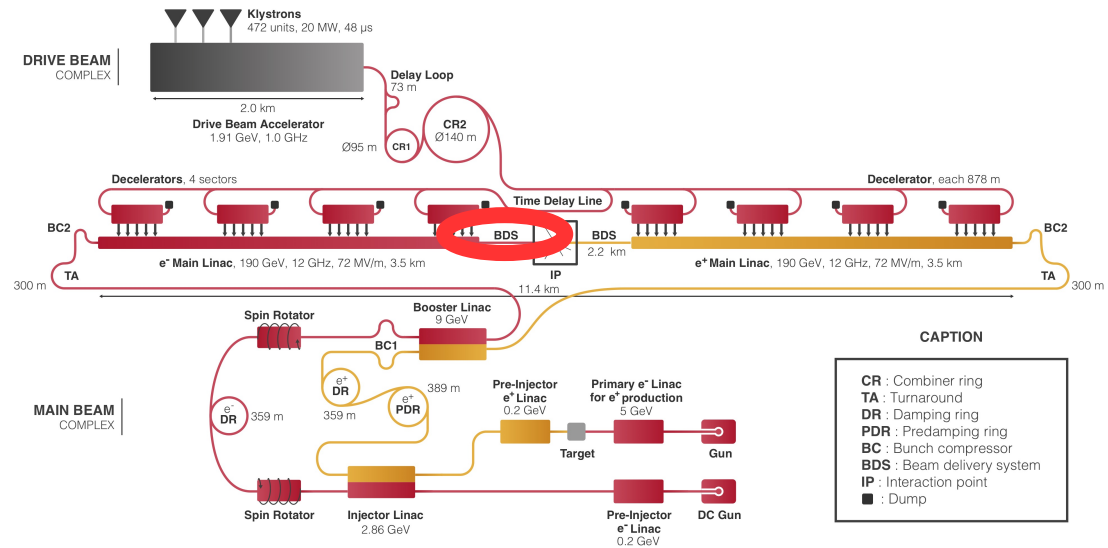
The Compact Linear Collider

CLIC is a global collaboration of more than 70 institutes and laboratories from more than 30 countries around the world. The CLIC concept was initiated at CERN, however, the theory and the technology are being developed and tested at member institutes worldwide.



Introduction

The CLIC Beam Delivery System (BDS)



380 GeV

Table: CLIC 380 GeV beam parameters.

Parameter	Symbol	Value
Centre-of-mass energy	E_{CM}	380 GeV
Length of the BDS	L_{BDS}	1949 m
Number of bunches	n_b	352
Bunch population	N	$5.2 \times 10^9 e^-$
RMS bunch length	σ_z	70 μ m
Bunch separation	Δt_b	0.5 ns
IP RMS beam sizes	σ_x^*/σ_y^*	149/2.9 nm

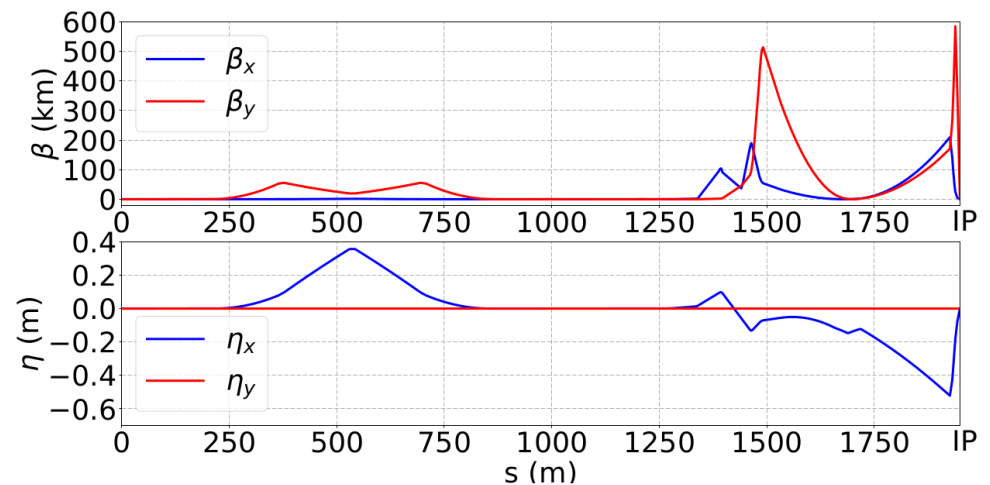


Figure: CLIC BDS 380 GeV Twiss parameters calculated with PLACET.

Simulations of the impact of short-range wakefields in CLIC

Impact of corrections and intensity dependent effects

Impact of corrections in CLIC

Simulation conditions (1/2)

Simulated errors:

- Static errors:
 - Misalignment of quadrupoles, sextupoles and BPMs of $50\ \mu\text{m}$ RMS.
 - Strength error of quadrupoles and sextupoles of 0.1% RMS.
 - Roll error for quadrupoles and sextupoles of $200\ \mu\text{rad}$ RMS.

Corrections applied:

- One-to-one
- DFS
- WFS
- Knobs (Y, YP D XP XP.*XP XP.*YP XP.*D)


Simulation procedure:

- 100 machines with the previously cited static imperfections.
- Apply the cited corrections and the knobs on the distribution at the IP.
- Measure the vertical beam size at the IP.

Impact of corrections in CLIC Simulation conditions (2/2)

Wakefield sources: X-band cavity BPMs (C-BPMs), wakepotentials calculated with GdfidL.

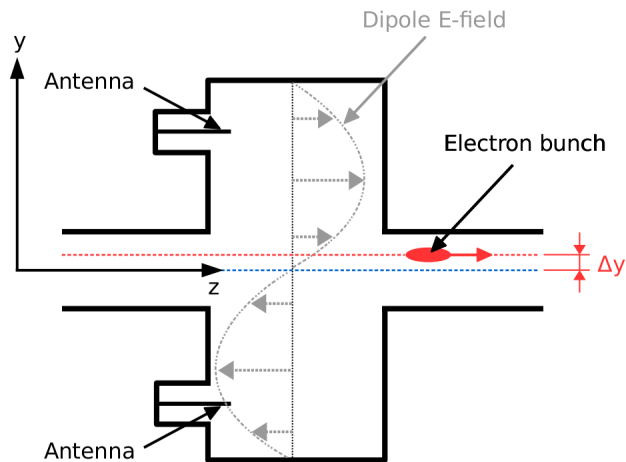


Figure: Schematic of a C-BPM.

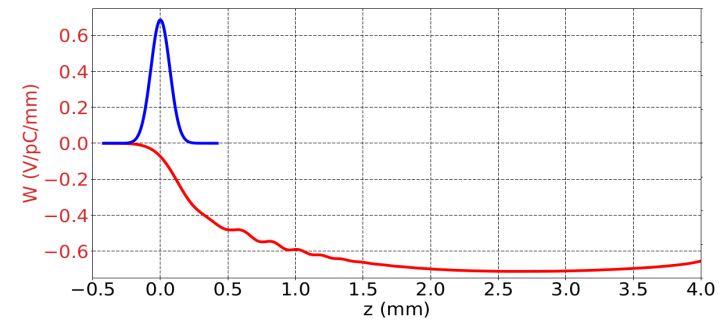


Figure : Transverse wakepotential in V/pC/mm of the CLIC C-BPM, calculated with GdfidL for a vertical offset of 1 mm, Gaussian bunch length of 70 μm and 1 pC charge (in red). For reference, the distribution of the electrons in one bunch is shown (in blue).

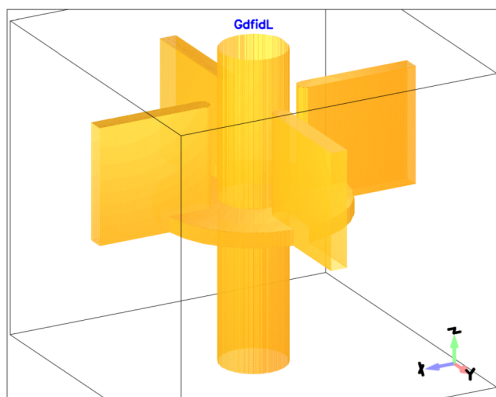


Figure: Geometry of the CLIC C-BPM, generated with GdfidL.

Table: Positions of CLIC 380 GeV BDS C-BPMs.

#	s (m)	#	s (m)	#	s (m)	#	s (m)	#	s (m)
1	0.0	28	158.9	55	868.4	82	971.4	109	1131.2
2	5.5	29	159.4	56	868.9	83	979.8	110	1131.7
3	11.0	30	178.1	57	869.5	84	980.3	111	1140.1
4	16.5	31	178.6	58	870.0	85	998.4	112	1147.0
5	17.0	32	197.2	59	870.6	86	998.9	113	1159.5
6	26.4	33	202.0	60	871.1	87	999.8	114	1172.0
7	36.3	34	205.0	61	871.8	88	1000.3	115	1184.3
8	36.8	35	211.0	62	872.3	89	1018.4	116	1193.0
9	40.3	36	212.3	63	884.4	90	1018.9	117	1205.9
10	40.8	37	363.5	64	884.9	91	1027.3	118	1218.8
11	44.4	38	364.8	65	885.5	92	1027.8	119	1231.2
12	44.9	39	376.0	66	886.0	93	1036.2	120	1246.8
13	48.5	40	377.3	67	886.9	94	1036.7	121	1279.9
14	49.0	41	528.5	68	887.4	95	1054.8	122	1333.9
15	52.5	42	529.8	69	905.5	96	1055.3	123	1337.1
16	53.0	43	541.0	70	906.0	97	1056.2	124	1391.0
17	62.4	44	542.3	71	914.4	98	1056.7	125	1394.2
18	62.9	45	693.5	72	914.9	99	1074.8	126	1460.6
19	72.3	46	694.8	73	923.3	100	1075.3	127	1463.8
20	72.8	47	706.0	74	923.8	101	1083.7	128	1483.6
21	82.2	48	707.3	75	941.9	102	1084.2	129	1488.6
22	101.3	49	858.5	76	942.4	103	1092.6	130	1658.2
23	101.8	50	859.8	77	943.4	104	1093.1	131	1687.4
24	120.5	51	866.1	78	943.9	105	1111.2	132	1716.7
25	121.0	52	866.6	79	961.9	106	1111.7	133	1925.7
26	139.7	53	867.3	80	962.4	107	1112.6	134	1938.4
27	140.2	54	867.8	81	970.9	108	1113.1		

The short-range wakefield sources taken into account are the 134 CLIC C-BPMs.

Impact of corrections in the CLIC 380 GeV BDS

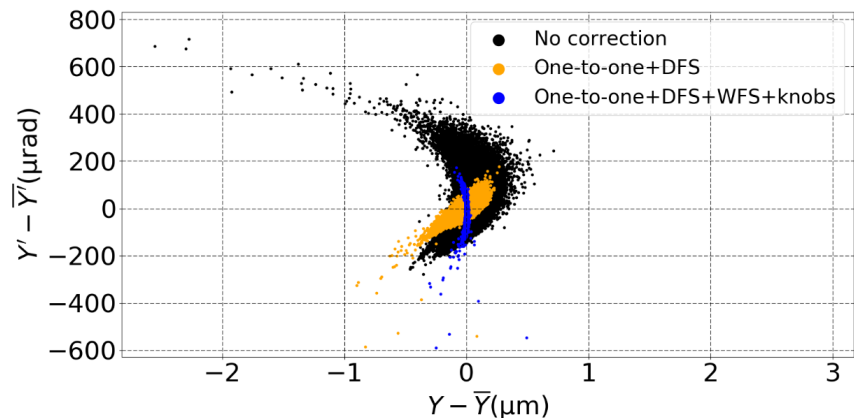


Figure 1: Centered vertical phase space at the 380 GeV CLIC BDS IP, $Y' - \bar{Y}'$ vs. $Y - \bar{Y}$, for 3 cases: no correction, One-to-one steering, DFS, WFS and One-to-one steering, DFS, WFS and knobs, calculated with PLACET with wakefields.

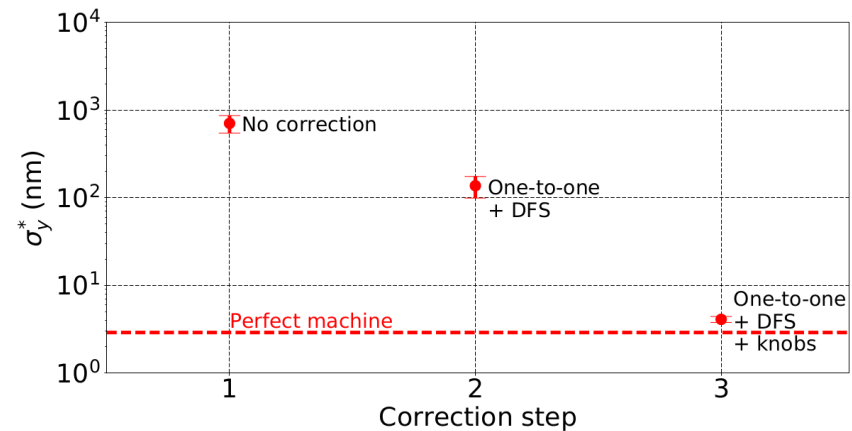


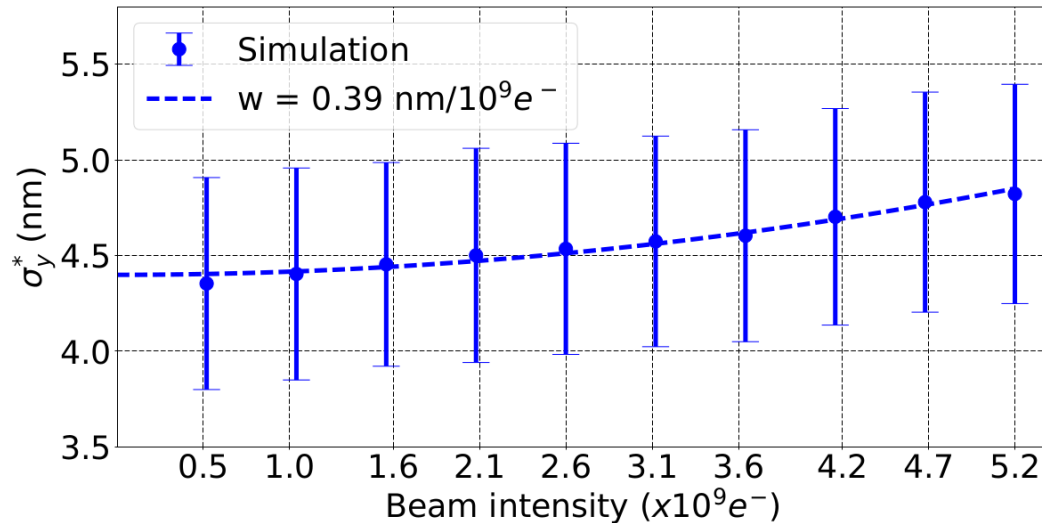
Figure 2: Average vertical beam size at the 380 GeV CLIC IP (σ_y^*) vs. correction step: One-to-one, DFS, WFS corrections and IP tuning knobs. The red dashed line show the vertical beam size at the IP for a perfect machine, 2.9 nm, calculated with PLACET with wakefields.

Table 1: Impact of the corrections on the CLIC 380 GeV vertical beam size at the IP (σ_y^*) for 100 machines with wakefields and with a beam intensity of $5.2 \times 10^9 e^-$, calculated with PLACET with wakefields.

Correction	$\overline{\sigma_y^*}$
No correction	706 ± 160 nm
One-to-one + DFS	$137 \pm 38,0$ nm
One-to-one + DFS + knobs	4.82 ± 0.570 nm

Orbit corrections and knobs reduce the beam size by a factor 147.

Impact of short-range wakefields in the CLIC 380 GeV BDS



$$w [nm/10^9 e^-] = \frac{(\sqrt{\sigma_{y,q}^2 - \sigma_{y,0}^2})}{q}$$

Figure 1: Vertical IP beam size σ_y^* vs. beam intensity in the 380 GeV BDS, calculated with PLACET with wakefields.

Table 1: Intensity-dependent effects due to wakefields on the vertical IP beam size (σ_y^*) in the 380 GeV BDS, calculated with PLACET with wakefields.

Beam intensity	$\overline{\sigma_y^*}$ (nm)	w (nm/10 ⁹ e ⁻)
$5.2 \times 10^8 e^-$	4.35 ± 0.55	0.39
$5.2 \times 10^9 e^-$	4.82 ± 0.57	

Short-range wakefields have a slight effect in the 380 GeV BDS.

Simulations of the impact of long-range wakefields in CLIC

In the CLIC 380 GeV BDS

Long-range wakefields in the CLIC BDS

Resistive walls wakefield

- Electrons going through the pipe interacts with the surrounding structure and generates a wake field.
- This wake field produces a transverse kick for the following bunches.
- The following model is used for the transverse wake function [11]:

$$W(z) = \frac{c}{\pi b^3} \sqrt{\left(\frac{Z_0}{\sigma_r \pi z}\right) L}$$

With b the radius of the beam pipe, Z_0 the impedance of the vacuum, σ_r the conductivity of the pipe and L the length of the beam line element.

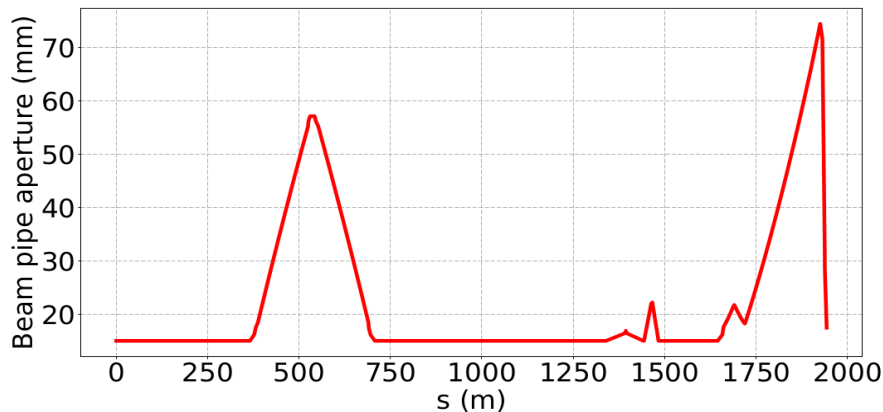
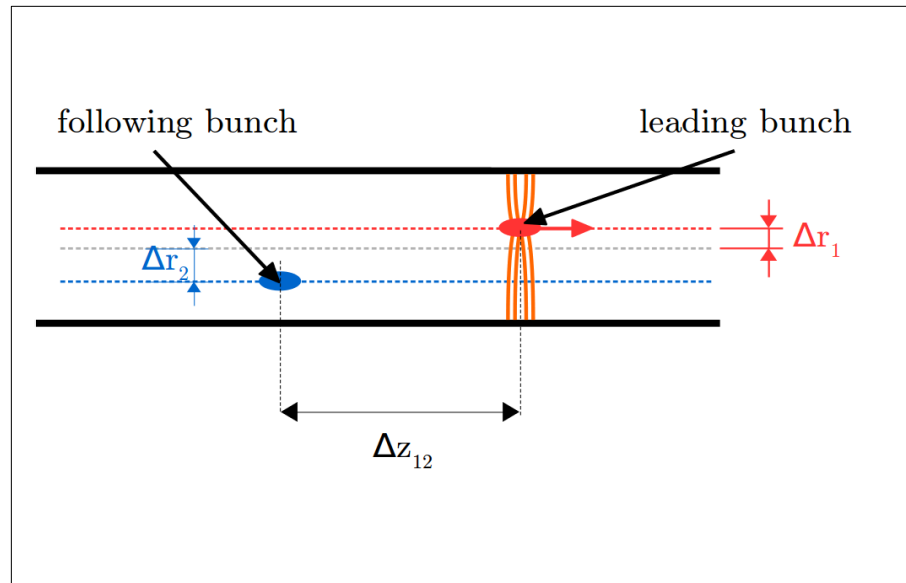


Figure: The CLIC BDS beam aperture profile.

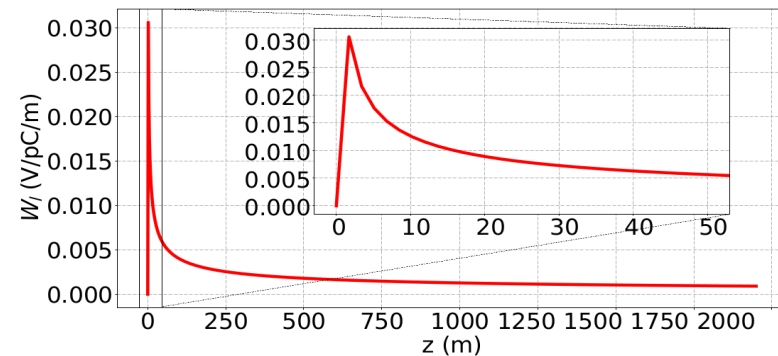


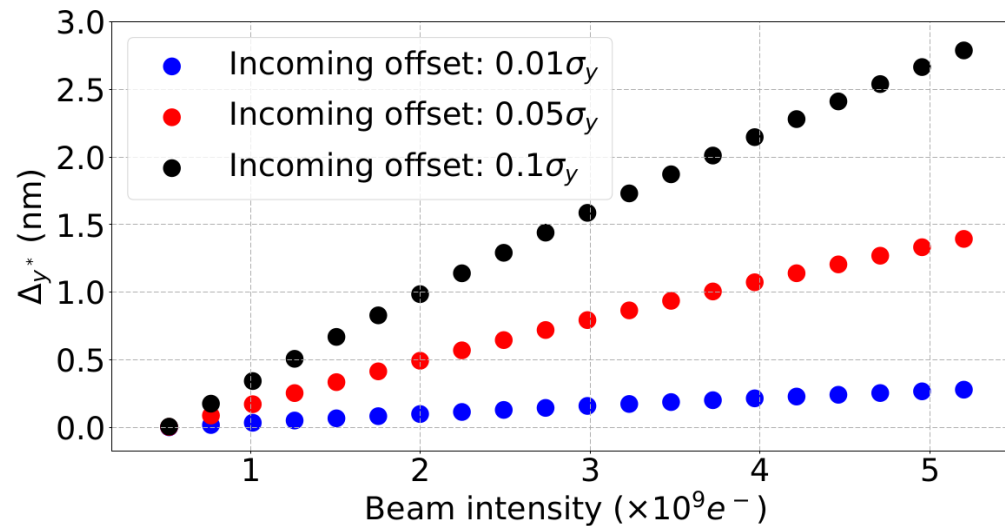
Figure : The CLIC resistive walls wakepotential for a copper beam pipe with a constant radius of 15 mm for the length of the CLIC BDS (~1949 m). The zoom shows the wakepotential for the length of a train (~52.8 m).

The long-range wakefield sources taken into account are the resistive walls.

Impact of long-range wakefields in the CLIC 380 GeV BDS for a constant offset

Simulation procedure:

- A train of 352 bunches is injected at the entrance of the BDS.
- Each bunch is made of one macro-particle.
- Incoming position and angle offset of the train to study the impact of long-range wakefields. Amplitude of the incoming offsets: $0.01\sigma_y$, $0.05\sigma_y$, $0.1\sigma_y$ or σ_y , with σ_y and σ_y' , the beam size and the beam divergence at the entrance of the BDS.



$$\sigma_y = 0.66 \mu m$$
$$\sigma_{y'} = 0.14 \mu rad$$

Figure : Vertical orbit deflection at the IP between the first and last bunch of a train Δy^* vs. beam intensity for three incoming constant position offsets of the train of bunches in the 380 GeV CLIC BDS: $0.01\sigma_y$, $0.05\sigma_y$ and $0.1\sigma_y$, calculated with PLACET with resistive walls.

Impact of long-range wakefields in the CLIC 380 GeV BDS for a constant offset

- Study of the impact of long-range wakefields for a train injected in the BDS with a constant vertical position and an angle offset of $0.01\sigma_y$ and $0.01\sigma_{y'}$, respectively on the vertical orbit deflection at the IP normalised by the IP beam size, $\Delta y^*/\sigma_y^*$ (left).
- Same study was done for both vertical and horizontal incoming offsets (right).

$$\sigma_{y'} = 0.14 \mu\text{rad} \quad \sigma_y = 0.66 \mu\text{m} \quad \sigma_y^* = 2.9 \text{ nm}$$

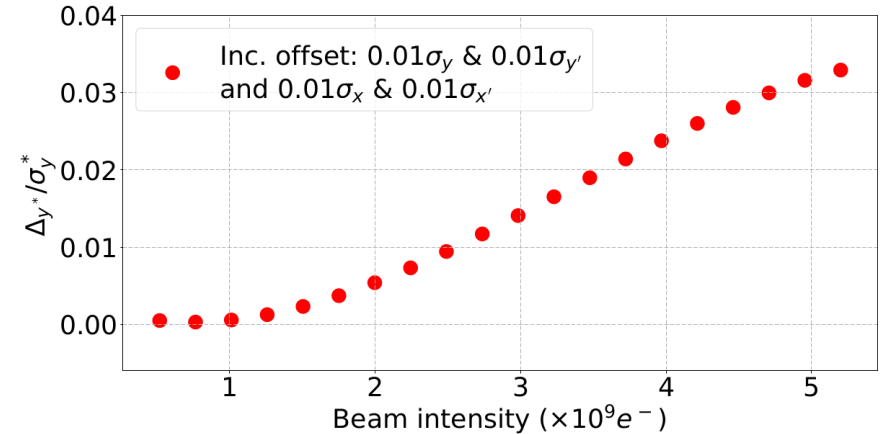
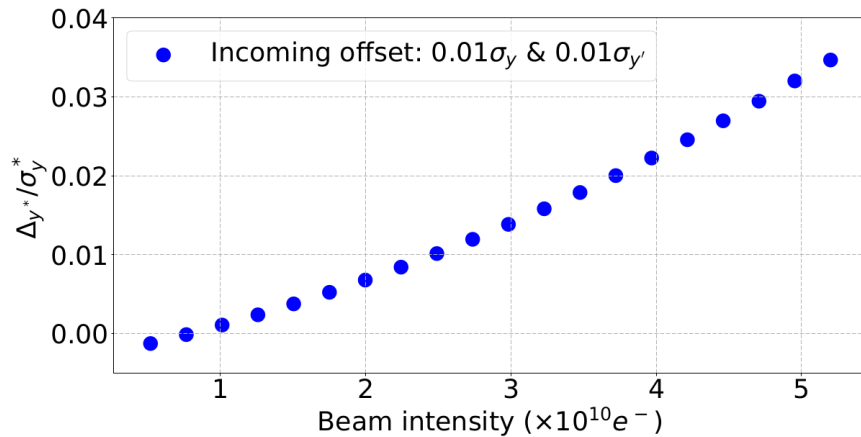


Figure 1: Vertical orbit deflection at the IP between the first and last bunch of a train normalised by the IP vertical beam size ($\Delta y^*/\sigma_y^*$) vs. beam intensity for a train with incoming constant horizontal position and angle offsets of respectively $0.01\sigma_x$ and $0.01\sigma_{x'}$ and vertical incoming position and angle offsets of respectively $0.01\sigma_y$ and $0.01\sigma_{y'}$ in the 380 GeV BDS, calculated with PLACET with resistive walls.

Figure 2: Vertical orbit deflection at the IP between the first and last bunch of a train normalised by the IP vertical beam size ($\Delta y^*/\sigma_y^*$) vs. beam intensity for a train with incoming constant horizontal position and angle offsets of respectively $0.01\sigma_x$ and $0.01\sigma_{x'}$ and vertical incoming position and angle offsets of respectively $0.01\sigma_y$ and $0.01\sigma_{y'}$ in the 380 GeV CLIC BDS, calculated with PLACET with resistive walls.

Impact of long-range wakefields in the CLIC 380 GeV BDS for a random offset

- Study of the impact of long-range wakefields for a train injected in the BDS with a random horizontal and vertical position and an angle offsets.
- The distribution of random incoming position and angle offset is a normal distribution with a zero mean and variance of 2.6×10^{-4} , leading to a $\pm 5\%$ incoming vertical and horizontal angle and position offsets.

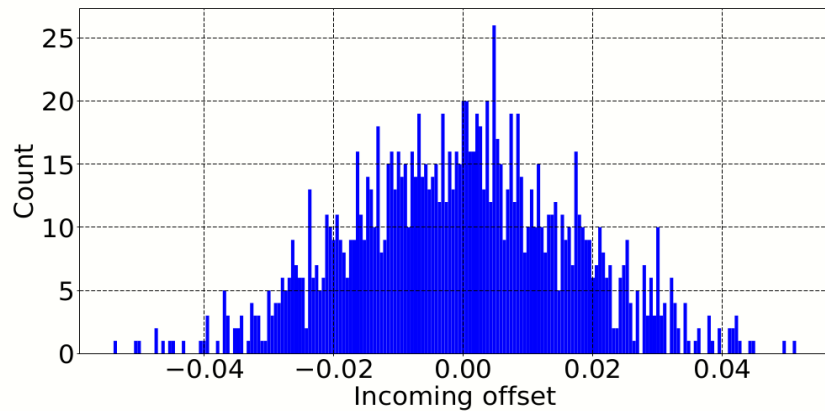
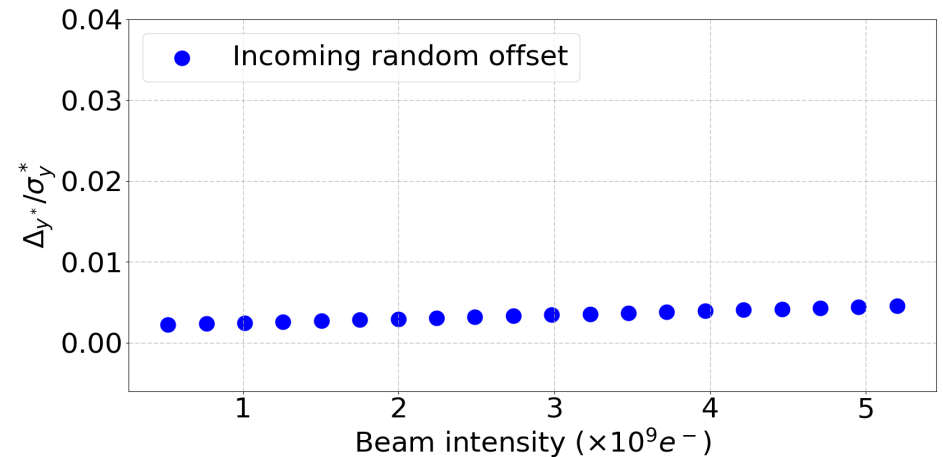


Figure : Distribution of incoming position and angle offsets from $-0.05\sigma_{x,y}$ to $0.05\sigma_{x,y}$.



Random incoming offsets lead to a negligible effect of long-range wakefields

Impact of long-range wakefields in the CLIC 380 GeV BDS Luminosity

- Study of the impact of luminosity degradation due to the vertical orbit deflection at the IP with Guinea-Pig, a code simulating the impact of beam-beam effects on luminosity and background [12].

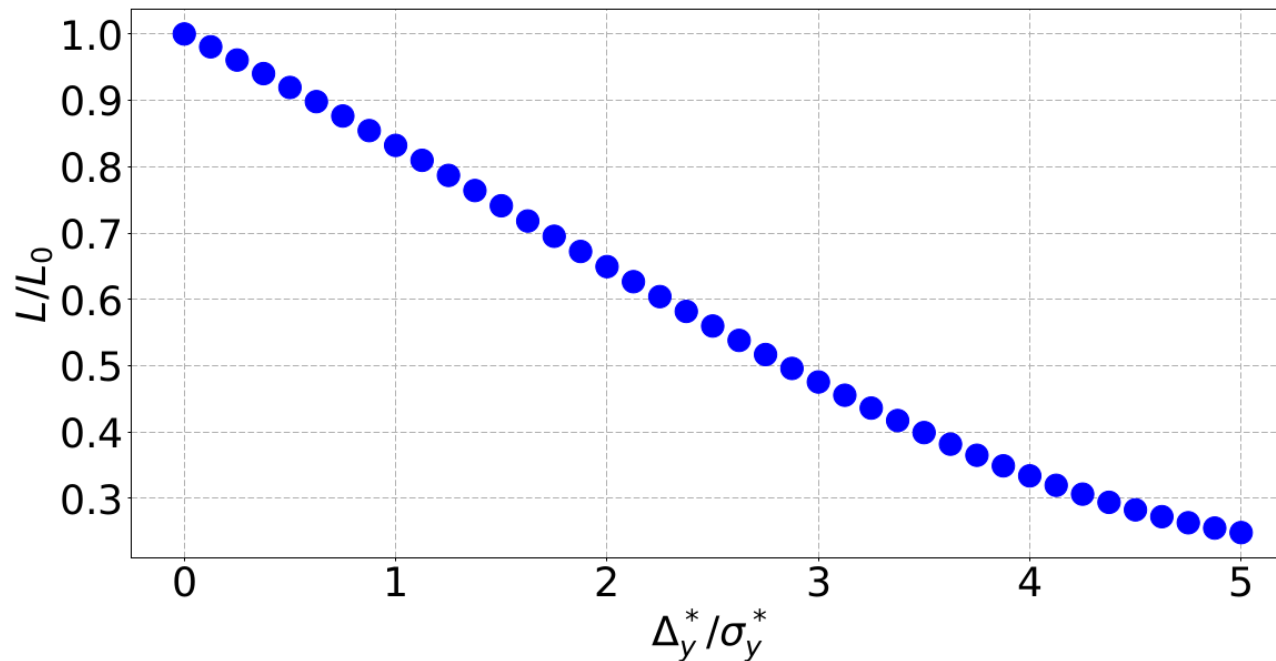


Figure : CLIC 380 GeV BDS luminosity degradation vs. relative vertical offset of the colliding beams.

$$L = f_{coll} \frac{n_1 n_2}{4\pi \sigma_x^* \sigma_y^*} F$$

Impact of long-range wakefields in the CLIC 380 GeV BDS Summary

Table : Impact of different incoming vertical position and angle offsets on the relative vertical offset Δ_y^* at the IP and the luminosity for low and high beam intensities in the CLIC 380 GeV BDS.

Case	Δ_y^* [nm]	Δ_y^*/σ_y^*	L/L_0
Inc. position offset $0.1\sigma_y$			
$0.52 \times 10^9 e^-$	0.006	0.002	~ 1.0
$5.2 \times 10^9 e^-$	2.79	0.96	0.84
Inc. angle offset $0.1\sigma_{y'}$			
$0.52 \times 10^9 e^-$	0.002	0.001	~ 1.0
$5.2 \times 10^9 e^-$	1.71	0.59	0.91
Inc. offsets $0.01\sigma_y$ & $0.01\sigma_{y'}$			
$0.52 \times 10^9 e^-$	0.003	0.001	~ 1.0
$5.2 \times 10^9 e^-$	0.087	0.03	~ 1.0
Inc. offsets $0.01\sigma_y$ & $0.01\sigma_{y'}$ and $0.01\sigma_x$ & $0.01\sigma_{x'}$			
$0.52 \times 10^9 e^-$	0.003	0.001	~ 1.0
$5.2 \times 10^9 e^-$	0.087	0.03	~ 1.0
Inc. random offsets around zero			
$0.52 \times 10^9 e^-$	0.006	0.002	~ 1.0
$5.2 \times 10^9 e^-$	0.015	0.005	~ 1.0

Long-range wakefields have a significant impact in the CLIC 380 GeV BDS. An intra-train feedback system would be necessary in order to achieve the luminosity goals.

Impact of short-range and long-range wakefields in the 500 GeV ILC BDS

Introduction

The International Linear Collider

The International Linear Collider (ILC) is a 250–500 GeV (extendable to 1 TeV) centre-of-mass high-luminosity linear electron-positron collider, based on 1.3 GHz superconducting radio-frequency accelerating technology. ILC parameters and technologies are summarized in the ILC Technical Design Report (2013) [13].

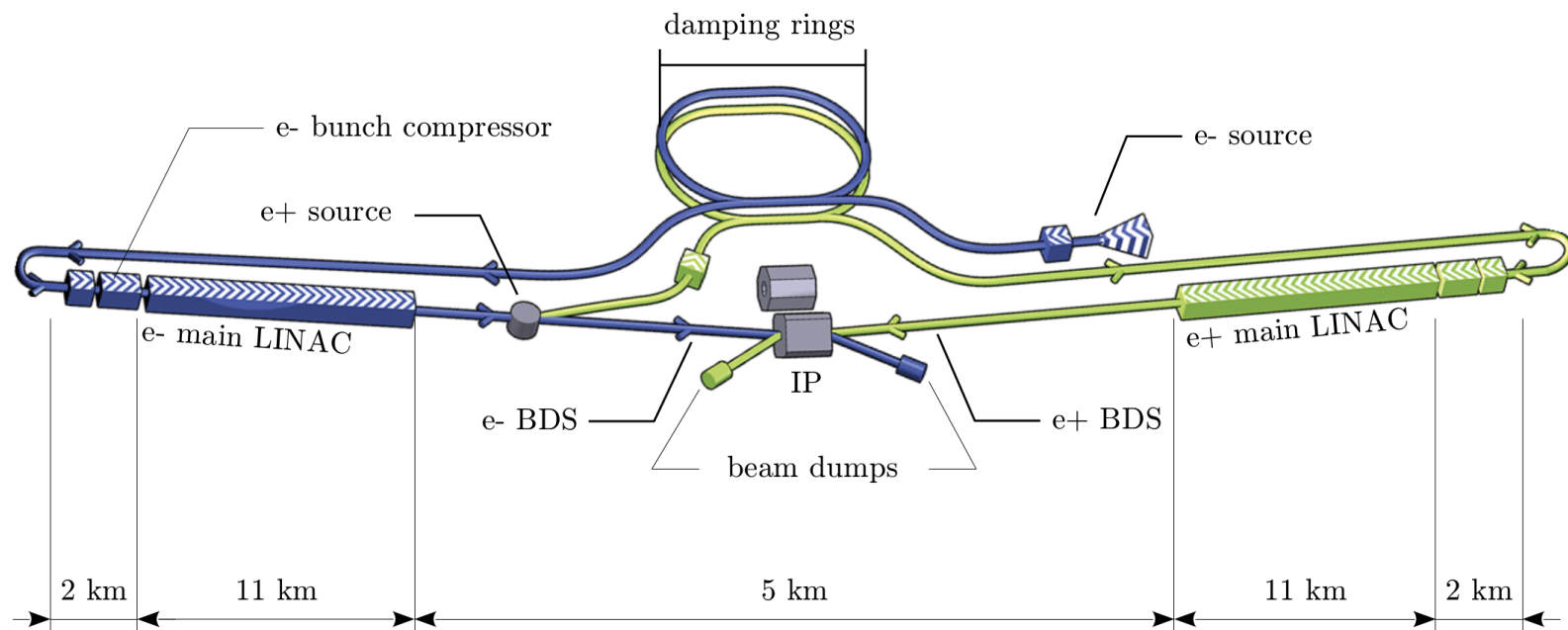


Figure: ILC 500 GeV layout with dimensions (not to scale)

Introduction

The ILC Beam Delivery System (BDS)

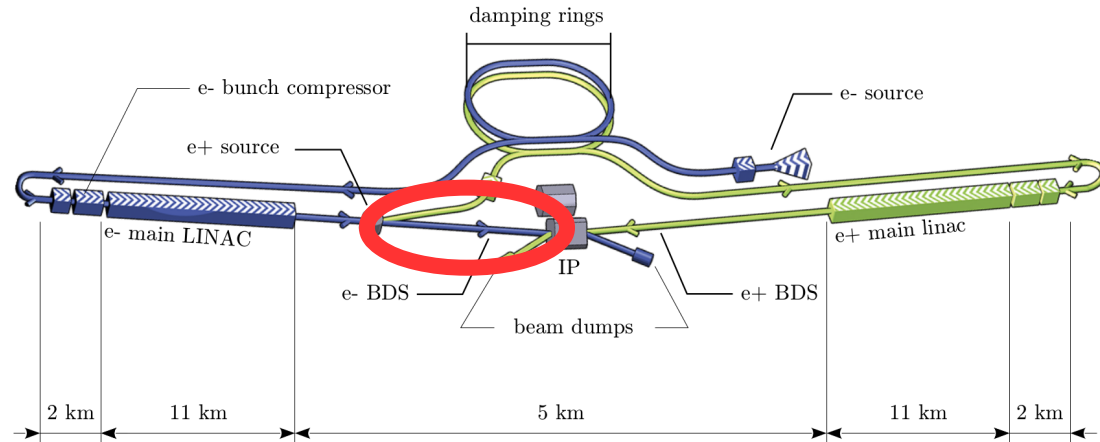


Table: ILC 250 GeV beam parameters.

Parameter	Symbol	Value
Centre-of-mass energy	E_{CM}	250 GeV
Length of the BDS	L_{BDS}	2254 m
Number of bunches	n_b	1312
Bunch population	N	$2.0 \times 10^{10} e^-$
RMS bunch length	σ_z	0.3 mm
Bunch separation	Δt_b	554 ns
IP RMS beam sizes	σ_x^*/σ_y^*	516/7.7 nm

Table: 500 GeV ILC beam parameters.

Parameter	Symbol	Value
Centre-of-mass energy	E_{CM}	500 GeV
Length of the BDS	L_{BDS}	2254 m
Number of bunches	n_b	1312
Bunch population	N	$2.0 \times 10^{10} e^-$
RMS bunch length	σ_z	0.3 mm
Bunch separation	Δt_b	554 ns
IP RMS beam sizes	σ_x^*/σ_y^*	474/5.9 nm

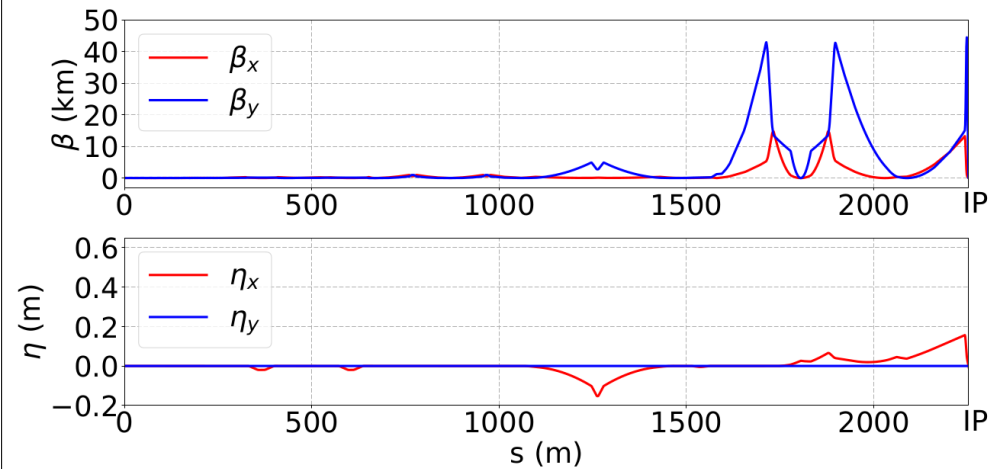


Figure: The ILC BDS 500 GeV Twiss parameters calculated with PLACET

Introduction

The ILC Beam Delivery System (BDS)

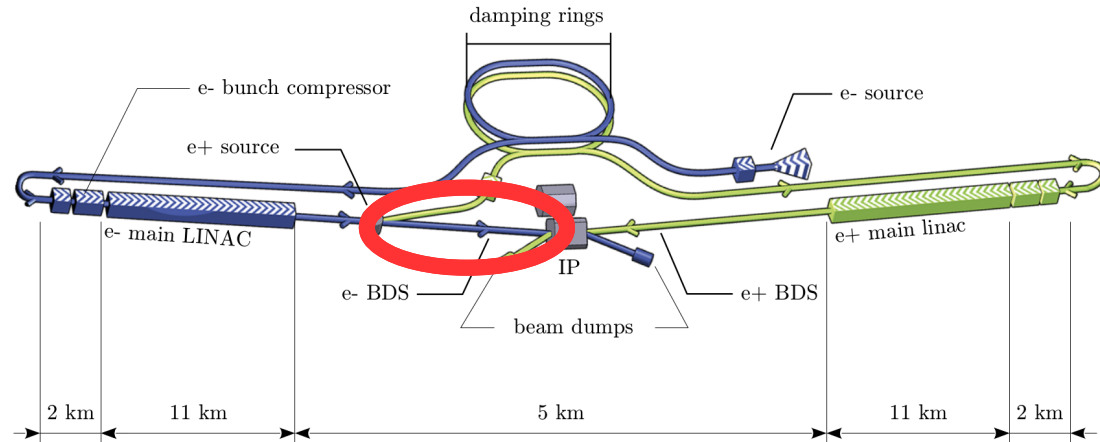


Table: ILC 250 GeV beam parameters.

Parameter	Symbol	Value
Centre-of-mass energy	E_{CM}	250 GeV
Length of the BDS	L_{BDS}	2254 m
Number of bunches	n_b	1312
Bunch population	N	$2.0 \times 10^{10} e^-$
RMS bunch length	σ_z	0.3 mm
Bunch separation	Δt_b	554 ns
IP RMS beam sizes	σ_x^*/σ_y^*	516/7.7 nm

Table: 500 GeV ILC beam parameters.

Parameter	Symbol	Value
Centre-of-mass energy	E_{CM}	500 GeV
Length of the BDS	L_{BDS}	2254 m
Number of bunches	n_b	1312
Bunch population	N	$2.0 \times 10^{10} e^-$
RMS bunch length	σ_z	0.3 mm
Bunch separation	Δt_b	554 ns
IP RMS beam sizes	σ_x^*/σ_y^*	474/5.9 nm

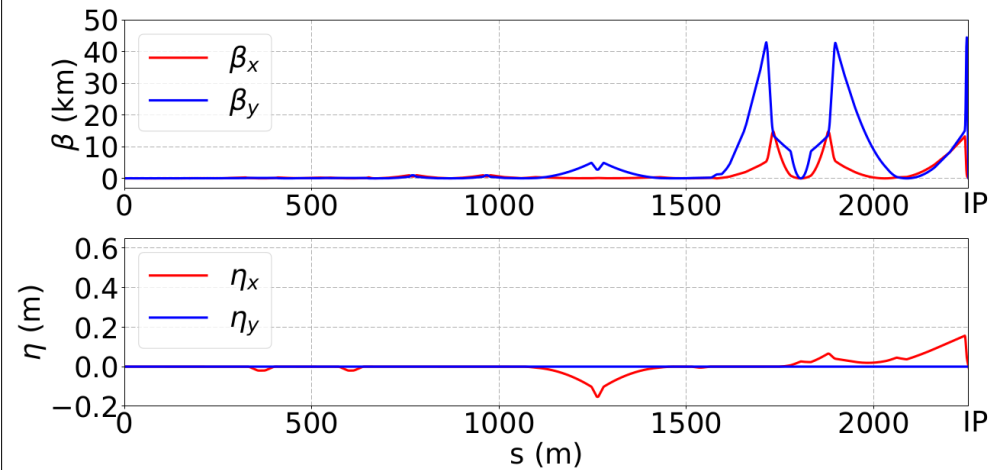


Figure: The ILC BDS 500 GeV Twiss parameters calculated with PLACET

Simulations of the impact of short-range wakefields in the ILC

Impact of corrections and intensity dependent effects

Impact of corrections in ILC

Simulation conditions (1/2)

Simulated errors:

- Static errors:
 - Misalignment of quadrupoles, sextupoles and BPMs of $50\ \mu\text{m}$ RMS.
 - Strength error of quadrupoles and sextupoles of 0.1% RMS.
 - Roll error for quadrupoles and sextupoles of $200\ \mu\text{rad}$ RMS.

Corrections applied:

- One-to-one
- DFS
- WFS
- Knobs (Y, YP D XP XP.*XP XP.*YP XP.*D)

First order Second order

Simulation procedure:

- 100 machines with the previously cited static imperfections.
- Apply the cited corrections and the knobs on the distribution at the IP.
- Measure the vertical beam size at the IP.

Impact of corrections in ILC Simulation conditions (2/2)

Wakefield sources: C-band cavity BPMs (C-BPMs), wakepotentials calculated with GdfidL.

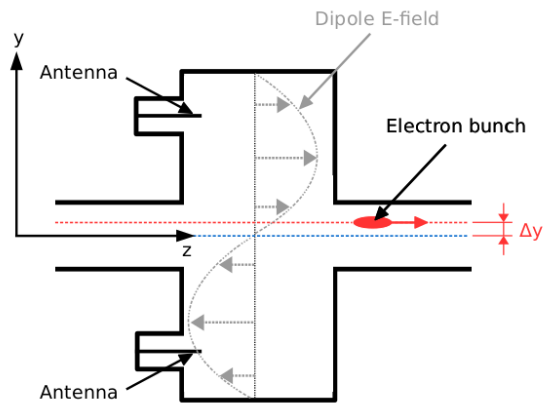
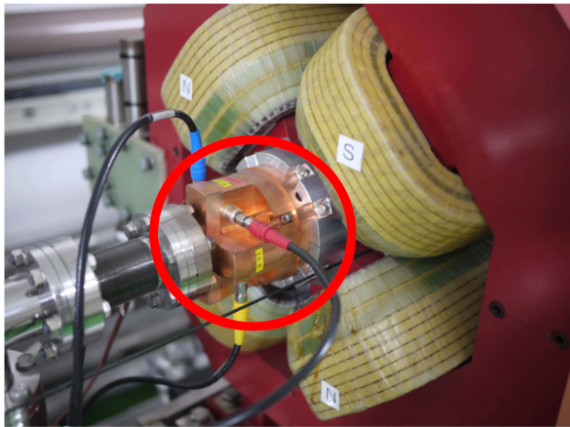


Figure: Picture of an ATF2 C-BPM (top) and schematic of a C-BPM (bottom).

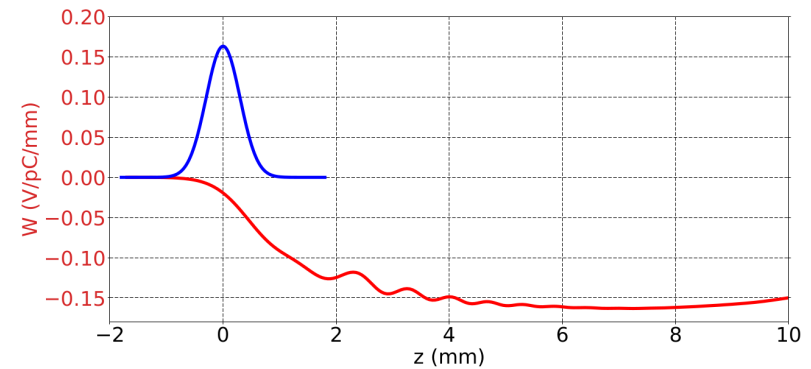


Figure : Transverse wakepotential in V/pC/mm of the ILC C-BPM, calculated with GdfidL for a vertical offset of 1 mm, Gaussian bunch length of 0.3 mm and 1 pC charge (in red). For reference, the distribution of the electrons in one bunch is shown (in blue).

Table: Positions of ILC BDS C-BPMs.

BPM #	s (m)	BPM #	s (m)	BPM #	s (m)	BPM #	s (m)
1	0.5	27	671.2	53	1247.1	79	1731.2
2	16.0	28	674.4	54	1261.1	80	1731.7
3	31.5	29	704.3	55	1265.1	81	1733.0
4	47.0	30	760.4	56	1279.1	82	1778.8
5	58.1	31	766.7	57	1429.0	83	1805.7
6	69.1	32	769.8	58	1468.2	84	1832.6
7	80.0	33	773.0	59	1481.0	85	1878.4
8	91.1	34	779.3	60	1495.0	86	1880.2
9	106.6	35	835.4	61	1509.0	87	1880.7
10	122.1	36	865.3	62	1510.7	88	1882.0
11	137.6	37	868.5	63	1537.9	89	1892.2
12	157.3	38	871.6	64	1565.1	90	1894.1
13	160.6	39	901.5	65	1566.7	91	1895.9
14	172.8	40	957.6	66	1580.7	92	1896.4
15	190.0	41	963.9	67	1594.7	93	1897.7
16	191.0	42	967.1	68	1607.9	94	2034.8
17	207.2	43	970.2	69	1614.9	95	2061.7
18	224.4	44	976.5	70	1654.4	96	2088.6
19	225.4	45	1013.8	71	1659.4	97	2242.8
20	241.6	46	1054.0	72	1697.6	98	2243.3
21	258.8	47	1058.0	73	1713.7	99	2243.4
22	259.8	48	1097.2	74	1715.5	100	2244.7
23	323.0	49	1135.4	75	1717.3	101	2247.4
24	326.5	50	1160.0	76	1719.2	102	2247.7
25	367.2	51	1184.6	77	1719.2	103	2247.7
26	466.5	52	1209.2	78	1729.4	104	2248.9

The short-range wakefield sources taken into account are the 104 ILC C-BPMs.

Impact of corrections in the ILC 250 and 500 GeV BDS

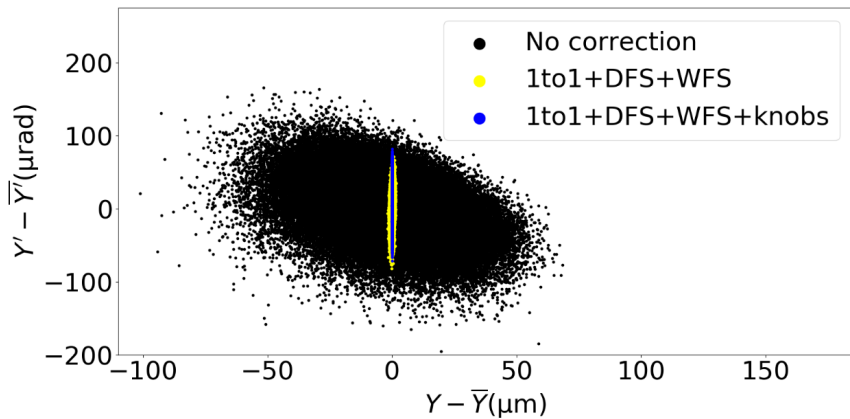


Figure 1: Centered vertical phase space at the 500 GeV ILC BDS IP, $Y' - \bar{Y}'$ vs. $Y - \bar{Y}$, for 3 cases: no correction, One-to-one steering, DFS, WFS and One-to-one steering, DFS, WFS and knobs, calculated with PLACET with wakefields.

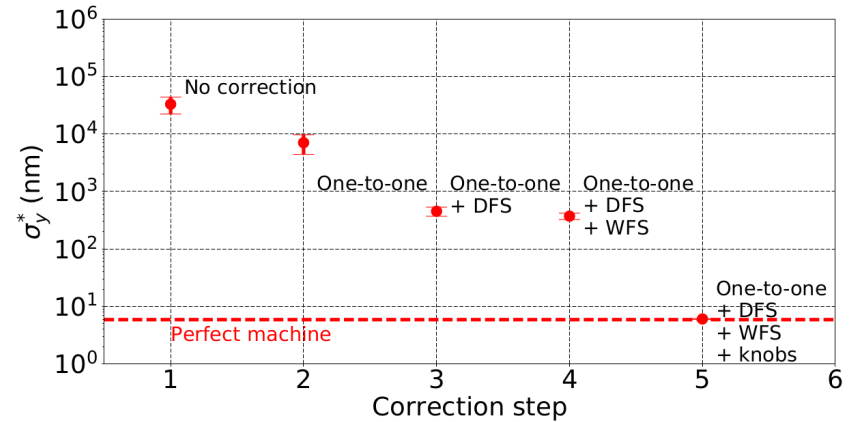


Figure 2: Average vertical beam size at the 500 GeV ILC IP (σ_y^*) vs. correction step: One-to-one, DFS, WFS corrections and IP tuning knobs. The red dashed line show the vertical beam size at the IP for a perfect machine, 5.9 nm.

Table 1: Impact of the corrections on the ILC 250 GeV vertical beam size at the IP (σ_y^*) for 100 machines with wakefields and $2 \times 10^{10} e^-$, simulated with PLACET.

Correction	$\bar{\sigma}_y^*$
No correction	$69.4 \pm 26.8 \mu\text{m}$
One-to-one	$1.1 \pm 0.3 \mu\text{m}$
One-to-one + DFS	$514 \pm 65 \text{ nm}$
One-to-one + DFS + WFS	$512 \pm 64 \text{ nm}$
One-to-one + DFS + WFS + knobs	$9.43 \pm 0.30 \text{ nm}$

Table 2: Impact of the corrections on the 500 GeV ILC vertical beam size at the IP (σ_y^*) for 100 machines with wakefields and $2 \times 10^{10} e^-$, simulated with PLACET.

Correction	$\bar{\sigma}_y^*$
No correction	$33.0 \pm 10.7 \mu\text{m}$
One-to-one	$7.1 \pm 2.6 \mu\text{m}$
One-to-one + DFS	$452 \pm 81 \text{ nm}$
One-to-one + DFS + WFS	$372 \pm 47 \text{ nm}$
One-to-one + DFS + WFS + knobs	$6.11 \pm 0.30 \text{ nm}$

Orbit corrections and knobs reduce the beam size by a factor 5400 for the 500 GeV case.

Impact of short-range wakefields in the 250 and 500 GeV BDS

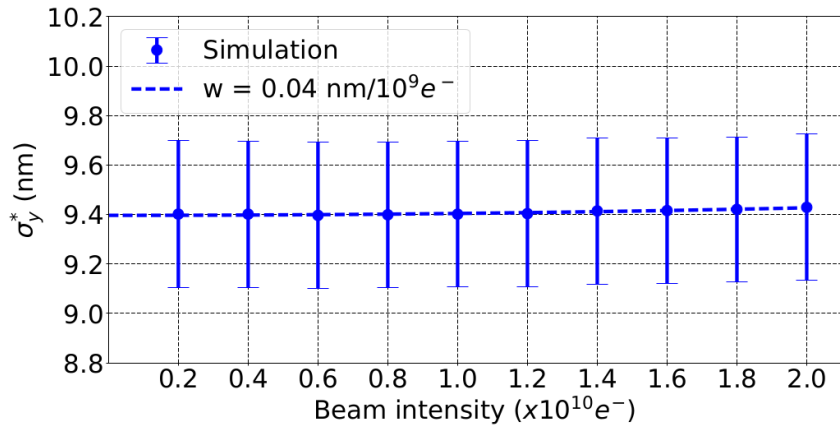


Figure 1: Vertical IP beam size σ_y^* vs. beam intensity in the 250 GeV BDS, calculated with PLACET with wakefields.

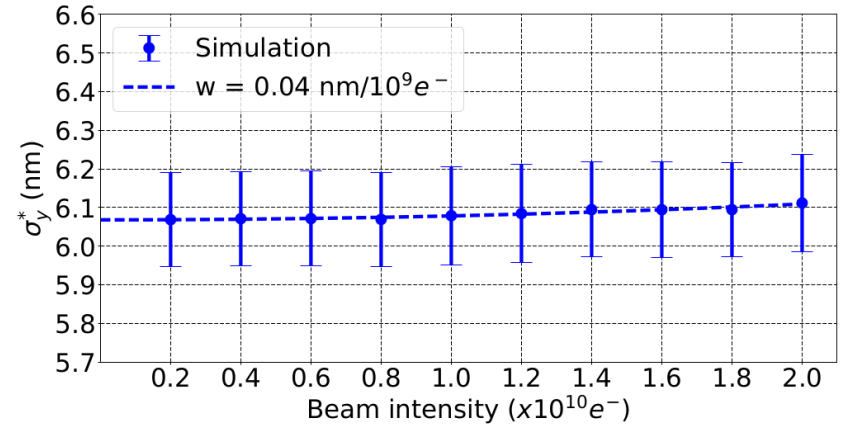


Figure 2: Vertical IP beam size σ_y^* vs. beam intensity in the 500 GeV BDS, calculated with PLACET with wakefields.

Table 1: Intensity-dependent effects due to wakefields on the vertical IP beam size σ_y^* in the 250 GeV ILC BDS, calculated with PLACET with wakefields.

Beam intensity	$\overline{\sigma_y^*}$ (nm)	w (nm/ $10^9 e^-$)
$0.2 \times 10^{10} e^-$	9.40 ± 0.30	0.04
$2.0 \times 10^{10} e^-$	9.43 ± 0.30	

Table 2: Intensity-dependent effects due to wakefields on the vertical IP beam size σ_y^* in the 500 GeV BDS, calculated with PLACET with wakefields.

Beam intensity	$\overline{\sigma_y^*}$ (nm)	w (nm/ $10^9 e^-$)
$0.2 \times 10^{10} e^-$	6.07 ± 0.30	0.04
$2.0 \times 10^{10} e^-$	6.11 ± 0.30	

Short-range wakefield effects are negligible in both 250 and 500 GeV BDS

$$w [nm/10^9 e^-] = \frac{(\sqrt{\sigma_{y,q}^2} - \sigma_{y,0}^2)}{q}$$

Simulations of the impact of long-range wakefields

In the 500 GeV ILC BDS

Long-range wakefields in the ILC BDS

Resistive walls wakefield

- Electrons going through the pipe interacts with the surrounding structure and generates a wake field.
- This wake field produces a transverse kick for the following bunches.
- The following model is used for the transverse wake function:

$$W(z) = \frac{c}{\pi b^3} \sqrt{\left(\frac{Z_0}{\sigma_r \pi z}\right)} L$$

With b the radius of the beam pipe, Z_0 the impedance of the vacuum, σ_r the conductivity of the pipe and L the length of the beam line element.

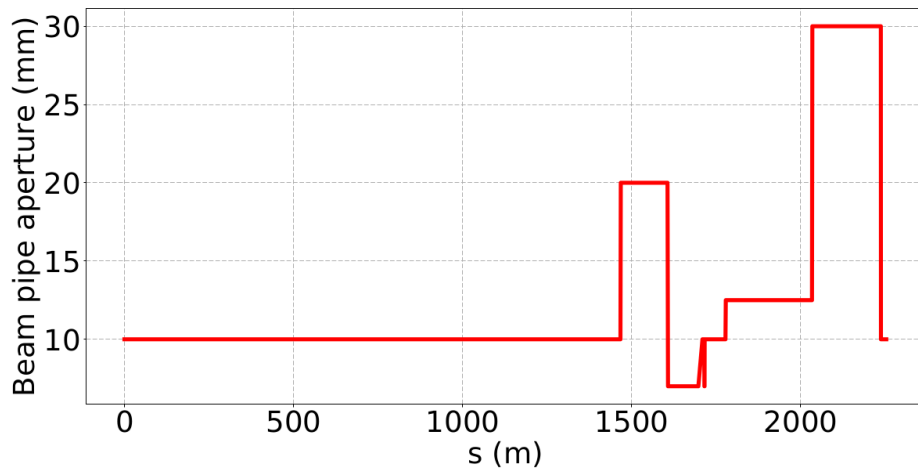
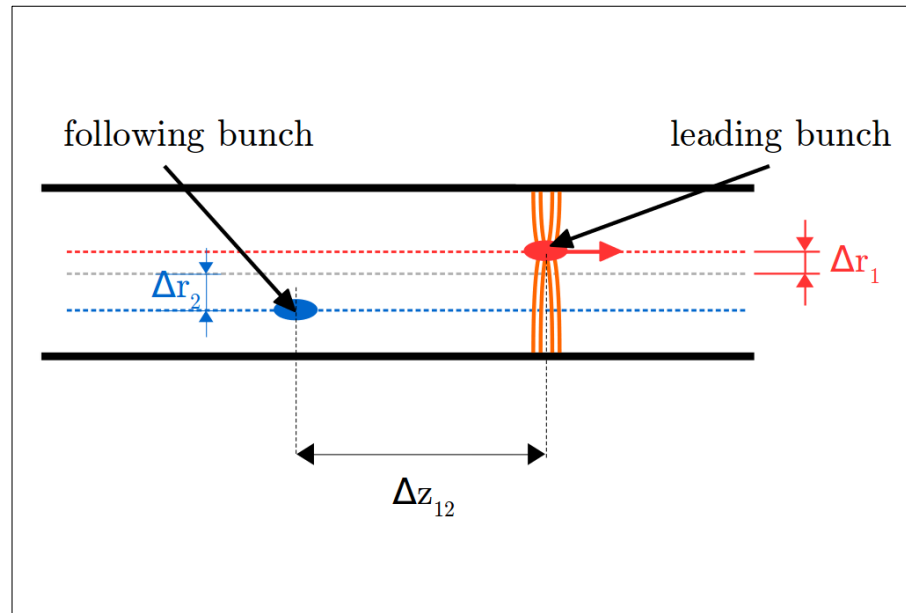


Figure: The ILC BDS beam aperture profile vs. s .

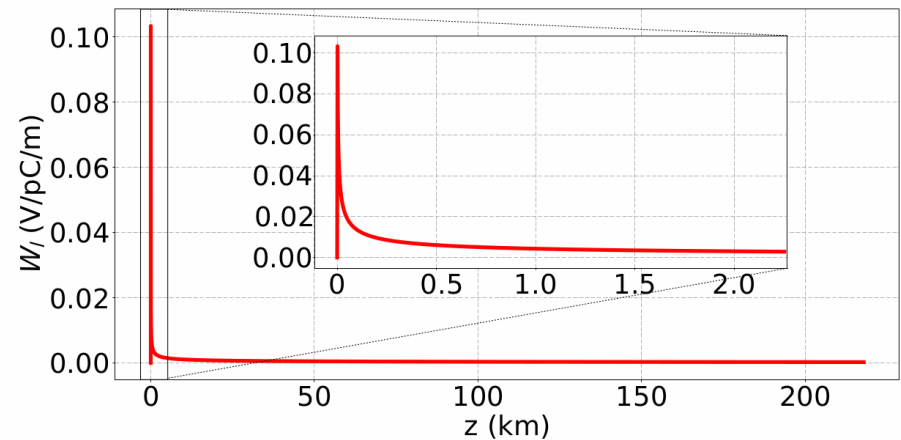


Figure : The ILC resistive walls wakepotential for a copper beam pipe with a constant radius of 10 mm for the length of a train (~ 218 km). The zoom shows the wakepotential for the length of the ILC BDS (~ 2254 m).

Impact of long-range wakefields in the 500 GeV ILC BDS

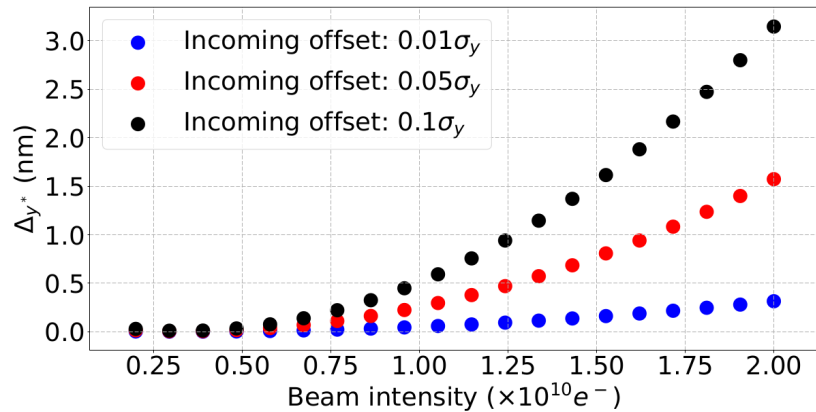


Figure 1: Vertical orbit deflection at the IP between the first and last bunch of a train Δy^* vs. beam intensity for three incoming constant position offsets of the train of bunches in the 500 GeV ILC BDS: $0.01\sigma_y$, $0.05\sigma_y$ and $0.1\sigma_y$, calculated with PLACET with resistive wall effects included.

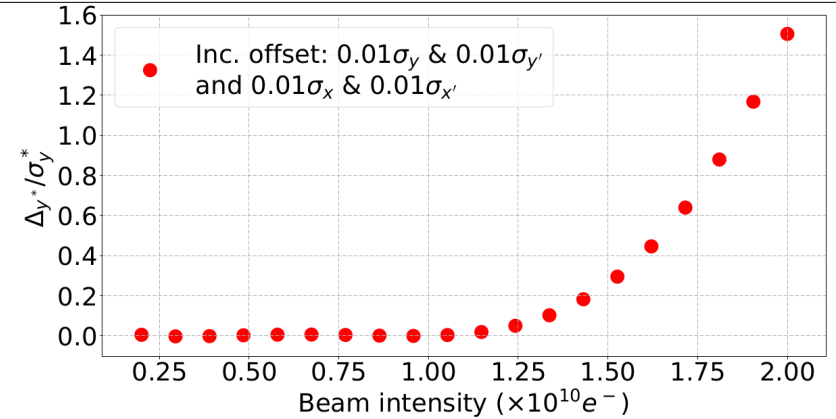


Figure 2: Vertical orbit deflection at the IP between the first and last bunch of a train normalised by the IP vertical beam size ($\Delta y^*/\sigma_y^*$) vs. beam intensity for a train with incoming constant horizontal position and angle offsets of respectively $0.01\sigma_x$ and $0.01\sigma_{x'}$ and vertical incoming position and angle offsets of respectively $0.01\sigma_y$ and $0.01\sigma_{y'}$ in the 500 GeV ILC BDS, calculated with PLACET with resistive wall effects included.

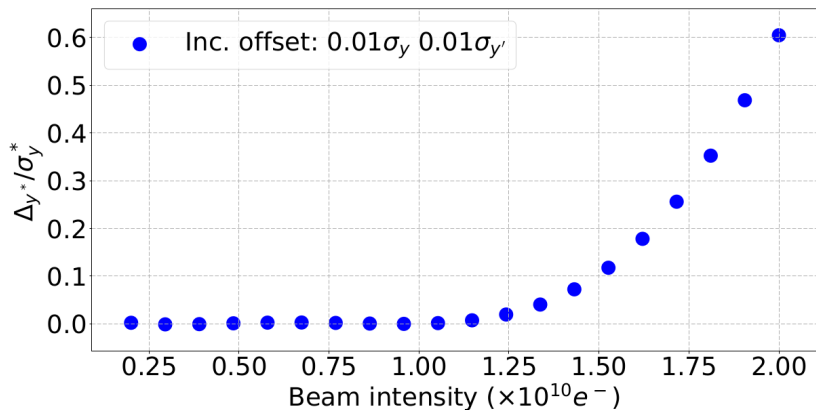


Figure 3: Vertical orbit deflection at the IP between the first and last bunch of a train normalised by the IP vertical beam size ($\Delta y^*/\sigma_y^*$) vs. beam intensity for a train with incoming constant position and angle offsets of respectively $0.01\sigma_y$ and $0.01\sigma_{y'}$ in the 500 GeV ILC BDS, calculated with PLACET with resistive wall effects included.

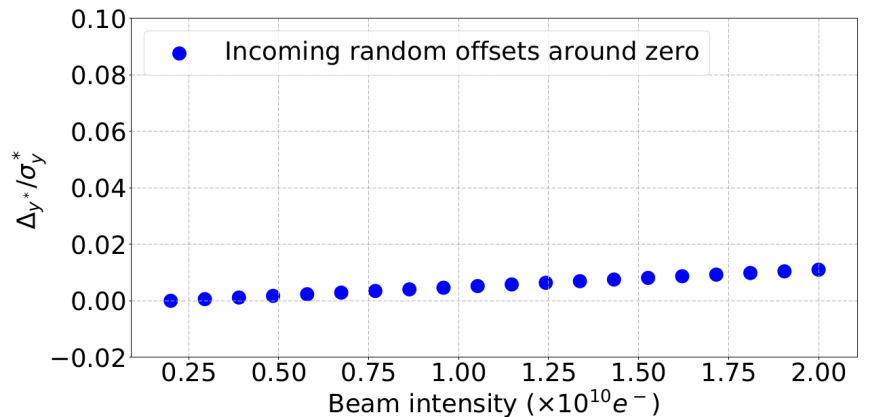


Figure 4: Vertical orbit deflection at the IP between the first and last bunch of a train normalised by the IP vertical beam size ($\Delta y^*/\sigma_y^*$) vs. beam intensity for a train with a random and around zero incoming vertical and horizontal position and angle offsets of between -0.05 and 0.05σ in the 500 GeV ILC BDS, calculated with PLACET with resistive wall effects included.

Impact of long-range wakefields in the 500 GeV ILC BDS Luminosity

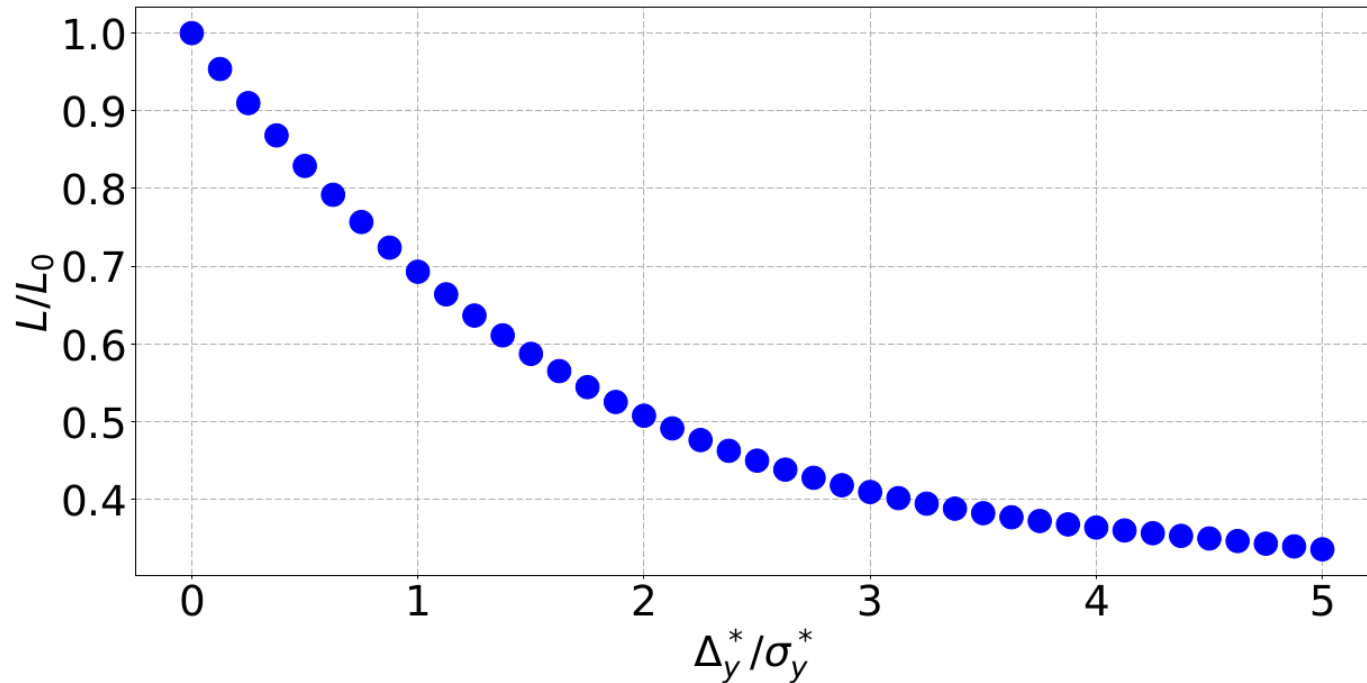


Figure : 500 GeV ILC BDS luminosity degradation vs. relative vertical offset of the colliding beams.

$$L = f_{coll} \frac{n_1 n_2}{4\pi \sigma_x^* \sigma_y^*} F$$

Impact of long-range wakefields in the 500 GeV ILC BDS Summary

Table : Impact of different incoming vertical position and angle offsets on the relative vertical offset Δ_y^* at the IP and the luminosity for low and high beam intensities in the ILC BDS 500 GeV.

Case	Δ_y^* [nm]	Δ_y^*/σ_y^*	L/L_0
Inc. position offset $0.1\sigma_y$			
$0.2 \times 10^{10} e^-$	0.028	0.005	~ 1.0
$2.0 \times 10^{10} e^-$	3.08	0.522	0.82
Inc. angle offset $0.1\sigma_{y'}$			
$0.2 \times 10^{10} e^-$	0.0178	0.003	~ 1.0
$2.0 \times 10^{10} e^-$	32.57	5.52	0.32
Inc. offsets $0.01\sigma_y$ & $0.01\sigma_{y'}$			
$0.2 \times 10^{10} e^-$	0.012	0.002	~ 1.0
$2.0 \times 10^{10} e^-$	3.54	0.6	0.80
Inc. offsets $0.01\sigma_y$ & $0.01\sigma_{y'}$ and $0.01\sigma_x$ & $0.01\sigma_{x'}$			
$0.2 \times 10^{10} e^-$	0.03	0.005	~ 1.0
$2.0 \times 10^{10} e^-$	8.91	1.51	0.59
Inc. random offsets around zero			
$0.2 \times 10^{10} e^-$	0.01	0.002	~ 1.0
$2.0 \times 10^{10} e^-$	0.06	0.01	~ 1.0

Long-range wakefields have a significant impact in the 500 GeV ILC BDS as well. An intra-train feedback system would be necessary in order to achieve the luminosity goals.

Acknowledgements

Special thanks to:

- Philip Burrows from the University of Oxford.
- Andrea Latina and Daniel Schulte from CERN.
- Angeles Faus-Golfe from IJCLab.
- Francois Meot and Guillaume Robert-Demolaize from BNL.

Conclusions – PhD Studies

- The intensity-dependent effects in ATF2 were quantified with PLACET taking into account several types of wakefield sources and considering realistic static and dynamic imperfections.
- The impact of several corrections (One-to-one, DFS, WFS, knobs) were studied with PLACET and showed promising results.
- The simulated and measured intensity-dependent parameters seemed to agree really well taking into account realistic simulation conditions in ATF2.
- The intensity-dependent effects due to short-range wakefields are negligible in both the CLIC and ILC BDS.
- The intensity-dependent effects due to long-range wakefields have a significant impact on the luminosity in both CLIC and ILC BDS.
- An intra-train feedback system is necessary in order to correct those effects and to achieve the required luminosity goals. Such a system has been studied to correct the vertical jitters generated by ground motion [14].
- A prototype feedback system was tested in ATF2 and gave promising results [15]. The next step will be to implement this feedback and study its impact on the luminosity losses due to intensity-dependent effects.

Thank you